

Cu-BTC metal-organic framework (MOF) as an efficient heterogeneous catalyst for BTC aerobic oxidative synthesis of imines from primary amines under solvent free conditions

Boosa Venu^a, Varimalla Shirisha^a, Bilakanti Vishali^a, Gutta Naresh^a, Ramineni Kishore^a, Inkollu Sreedhar^b and Akula Venugopal^{a,*}

^a Catalysis and Fine Chemicals Division, CSIR – Indian Institute of Chemical Technology, Tarnaka, Hyderabad – 500007, Telangana State, India. Corresponding author’s E-mail: akula@iict.res.in (Akula Venugopal). Tel: +91-40-27193165; Fax: +91-40-27160921.

^b Department of Chemical Engineering, BITS Pilani Hyderabad Campus, Hyderabad 500 078, Telangana State, India.

CSIR – IICT Communication number: IICT/Pubs./2019/189.

1 Experimental section.....	2-4
i). Characterization of catalysts/General methods	
ii). Preparation of TiO ₂ , Al ₂ O ₃ and SiO ₂ supported copper catalysts	
iii). Formula used for the normalized rate calculation	
2. General procedure for the synthesis of imine.....	4
3. Characterization of catalysts.....	4-14
i). Thermo gravimetric analysis (TGA)	
ii). Recyclability of Cu-BTC MOF catalyst	
iii). FT-IR spectroscopy	
iv). UV-DRS analysis of Cu-BTC MOF	
v). Transmission electron microscopic (TEM) analysis	
vi). BET surface areas of the catalysts	
vii). Formation of Cu ₃ (BTC) ₂	
viii). Effect of substrate ratio	
ix). Effect of catalyst amount	
x). Effect of reaction time	
xi). Large scale setup	
xii). XRD analysis	

xiii). N ₂ adsorption–desorption	
xiv). NH ₃ - temperature programmed desorption (TPD) analysis	
xv). Pyridine adsorbed DRIFT spectroscopy	
4. Spectral data of all products.....	14-22
5. References.....	23
6. ¹ H and ¹³ C NMR spectra	24-46

1. Experimental

i). Characterization of catalysts:

Purification of reaction products was carried out by flash chromatography using neutral alumina, and a mixture of ethyl acetate and petroleum ether as the eluting agent. ¹H NMR spectra were recorded by using Bruker VX NMR FT-300 or Varian Unity 500 and ¹³C NMR spectra were recorded by using Bruker VX NMR FT-75 MHz spectrometers instrument in CDCl₃. Chemical shifts (δ) are reported in ppm, using TMS as an internal standard. The surface properties of fresh samples were measured by N₂ adsorption at -196 °C, in an Autosorb 3000 physical adsorption apparatus. The specific surface areas were calculated applying the BET method. The fresh and used catalysts were characterized by powder XRD analysis using a Rigaku Miniflex X-ray diffractometer using Ni filtered Cu-Kα radiation (λ= 0.15406 nm) from 2θ = 20-80°, at a scan rate of 2° min⁻¹ with generator voltage and current of 30 kV and 15 mA respectively. The XPS patterns were recorded using a Kratos Axis Ultra Imaging X-ray photoelectron spectrometer, equipped with Mg anode and a multichannel detector. Charge referencing was done against adventitious carbon (C1s, 284.6 eV). A Shirley-type background was subtracted from the signals. The recorded spectra were fitted using Gauss-Lorentz curves to determine the binding energies of the different elements. The nature of acidic sites is investigated using pyridine adsorption in conjunction with FT-IR (Carry 660 equipped with mid-IR MCT detector; Agilent Technologies, USA). The spectra were collected in the range of 1400-1700 cm⁻¹ with a resolution of 4 cm⁻¹ and 64 no. of scans. The experiments were carried out using a DRIFT (Harrick) cell connected to a vacuum-adsorption set-

up. The catalyst samples were then pre-treated by heating them at 300 °C and maintained at the same temperature for 1 h. After cooling down to 150 °C, the spectrum was collected used as blank spectrum. Then the samples were exposed to pyridine (98%; Sigma-Aldrich) followed by vacuum for 30 minutes. The spectra obtained after pyridine adsorption subtracted from the blank spectrum. Finally, the resultant spectra were quantified using the Kubelka-Munk function. The inductively coupled plasma-optimal emission spectrophotometer (ICP-OES) analysis was carried out by using iCAP-6500 DUO, Thermo Fisher Scientifics UK. The SEM images were taken using FEI Nova 1200 NanoSEM instrument equipped with a TLD detector. The TGA analysis was performed on a Mettler Toledo apparatus. With a sample weight of ca 30-40 mg, the tests were performed under nitrogen flux in the temperature ranging from 25 to 800 °C and with the ramping rate of 10 °C/min.

ii). Preparation of TiO₂, Al₂O₃ and SiO₂ supported copper catalysts

The catalysts used in this study were prepared using the impregnation method with a copper nitrate aqueous solution to obtain catalysts with 5wt% copper supported on TiO₂, Al₂O₃ and SiO₂. Using the following procedure, 3 g of each catalyst was prepared. In typical synthesis procedure, corresponding weight percent of copper precursor (Cu(NO₃)₂ .3H₂O) was dissolved in deionized water by maintaining the homogeneity of the solution using magnetic stirring and required amount of support was added under vigorous stirring, while maintaining the temperature at 100 °C to evaporate the total solvent. The resultant solid was dried in an oven at 100 °C for 12 h and calcined at 450 °C for 5 h.

iii). Formula used for the normalized rate calculation (normalized with reaction temperature and reaction run time)

$$\text{Rate} = \frac{\text{Fractional yield} \times [\text{Substrate concentration}]}{g_{\text{Cu}}} \times \frac{1}{\text{Reaction run time (h)}} \times \frac{300 \text{ K}}{\text{Reaction temperature K}}$$

The rates are normalized with per gram of Cu in order to compare the product yields while correcting the rate with reaction time and reaction temperatures since various authors have conducted the aerobic oxidation of benzylamine reaction at various run times and temperatures.

2. General procedure for the synthesis of imines:

Benzylamine (7 mmol) and Cu-BTC MOF (~ 0.050 g) were placed in a round necked - bottomed flask fitted with a reflux condenser. The resulting reaction mixture was heated at 80 °C in an oxygen (balloon) atmosphere for a period of 12 h. After completion of the reaction monitored with TLC, 5 mL of ethyl acetate was added to the product mixture and then the catalyst was separated by centrifugation. The extracted ethyl acetate was concentrated under reduced pressure. However, the pure imine products were purified by column chromatographic separation using neutral alumina. The catalyst was washed with distilled water for several times then dried in an oven at 100 °C and used for the next cycle. Following the similar procedure, the aerobic oxidation of benzylamine reaction was tested for 5 recycles.

3. Characterization of catalysts:

i). Thermo gravimetric analysis (TGA):

Thermal stability of Cu-BTC is examined by thermo gravimetric analysis (TGA). The as synthesized Cu-BTC MOF was heated in nitrogen atmosphere with a heating rate of 5 °C min⁻¹. The thermogram shows three different regions viz., (1) the first weight loss (19.5%) in the region between 50 and 110 °C due to the loss of moisture, (2) the region between 110 to 290 °C is corresponding to the loss of two water molecules from the MOF with the weight loss of 6%. It is interesting to note that Cu co-ordination has been reduced from six to four at this stage, which is due to the color change during activation¹ and (3) the third region starts at 290 °C, at this temperature the of MOF structure is decomposed and the organic linker is buried. No weight loss beyond 315 °C is observed thus, explaining the Cu-BTC MOF sample is stable up to 300 °C.

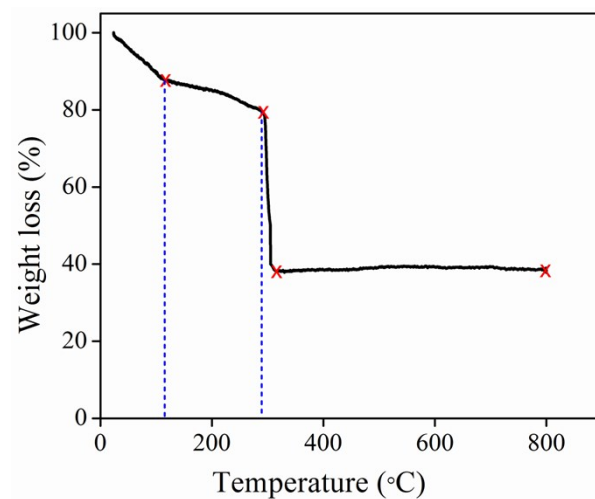


Fig. S1: Thermo-gravimetric analysis of Cu-BTC MOF sample.

ii). Recyclability of Cu-BTC MOF catalyst:

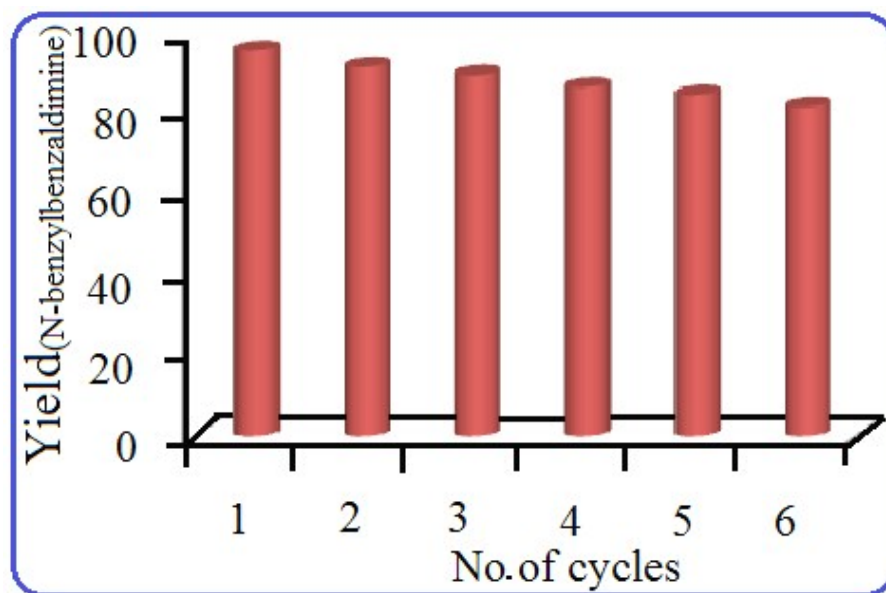


Fig. S2: Recyclability study over the Cu-BTC MOF catalyst.

iii). FT-IR spectroscopy

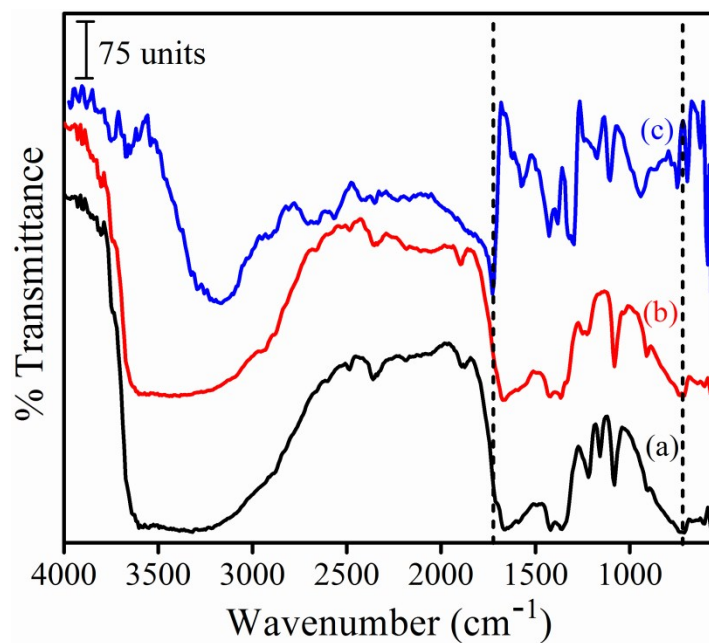


Fig. S3: FT-IR spectra of (a) fresh, (b) used Cu-BTC MOF and (c) 1,3,5-benzene tricarboxylic acid.

iv). UV-DRS analysis of Cu-BTC MOF:

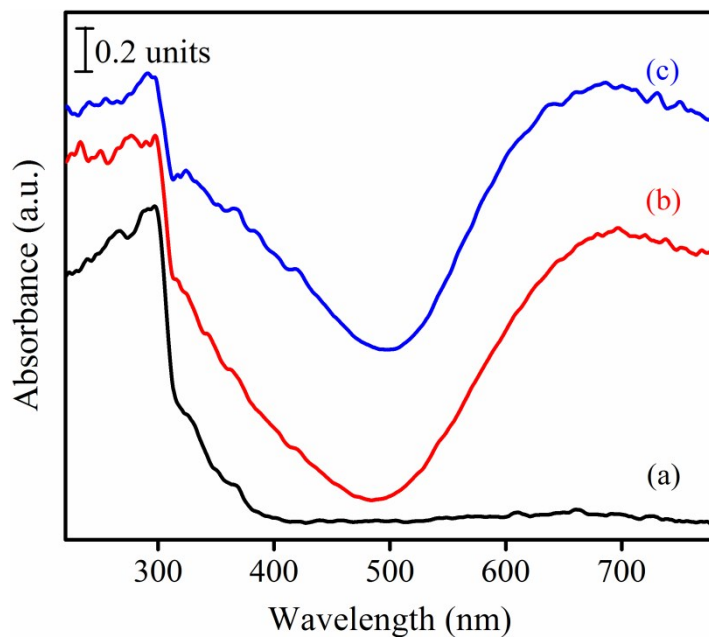


Fig. S4: UV-DRS spectra of (a) BTC, (b) Cu-BTC fresh and (c) Cu-BTC used catalysts.

V). Transmission electron microscopic (TEM) analysis:

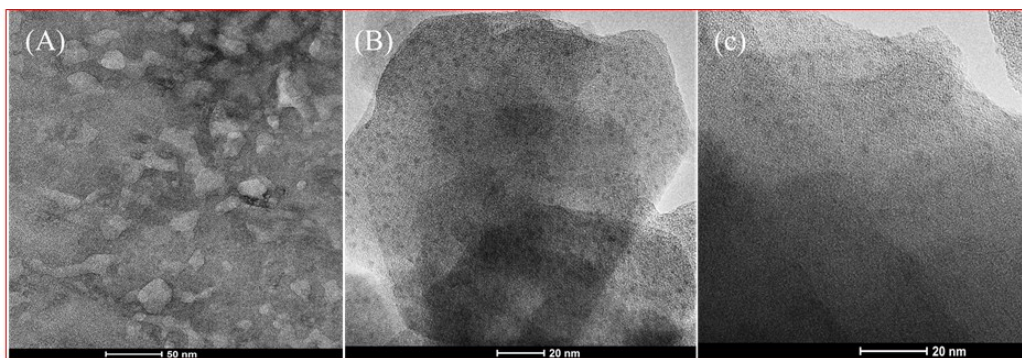


Fig. S5: TEM images of (A) and (B) fresh and (C) used Cu-BTC MOF samples.

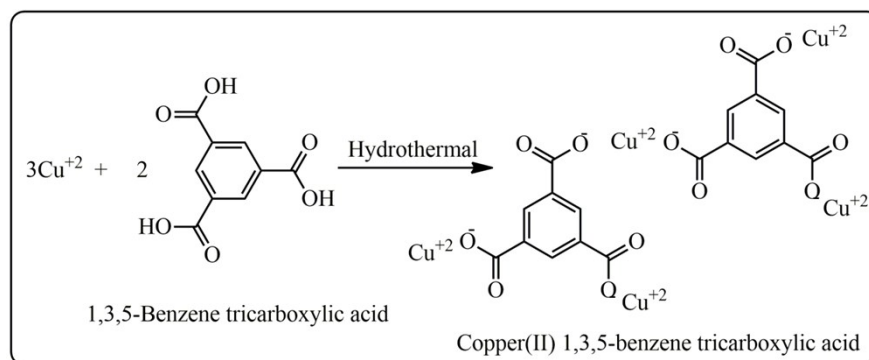
vi). BET surface areas of the catalysts.

Table S1: BET surface areas of the catalysts.

Catalyst	BET Surface area (m ² g ⁻¹)	Pore volume (cm ³ g ⁻¹)	Pore size (nm)
Cu-BTC - Fresh	620	0.37	2.43
Cu-BTC - Used	592	0.349	2.49
25wt%CuO/Al ₂ O ₃	210	0.42	8.9
25wt%CuO/TiO ₂	56	0.70	17.5
25wt%CuO/SiO ₂	390	0.32	5.8

^a Obtained from N₂-sorption analysis;

vii). Formation of Cu-BTC MOF:



Scheme S1: Reaction scheme for the synthesis of Cu-BTC MOF from 1,3,5-Benzene tricarboxylic acid.

viii). Effect of substrate ratio

The effect of benzylamine loading was studied using 1, 2, 3, 4, 5, 6 and 7 mmol under identical conditions which showed 30, 50, 72, 79, 85, 96 and 98% yields of the desired product respectively. Upon increasing the benzylamine substrate concentration from 1 to 7 mmol, the N-benzylbenzaldimine yield was increased from 30 to 98%. It was observed that when higher amount of benzylamine (6 mmol) used in the reaction mixture a higher yield of the desired product obtained. Further increase in the substrate concentration from 6 to 7 mmol, no appreciable change in the yield of the product is observed. Therefore, it is can be summarized that 6 mmol benzylamine was found to be optimum substrate ratio for the reaction under experimental conditions adopted in this study.

Table S2: Effect of substrate ratio on the aerobic oxidation of primary amines

S.No.	Substrate	Conc.	Yield(%)
1	Benzylamine	1 mmol	30
2	Benzylamine	2 mmol	50
3	Benzylamine	3 mmol	72
4	Benzylamine	4 mmol	79
5	Benzylamine	5 mmol	85
6	Benzylamine	6 mmol	96
7	Benzylamine	7 mmol	98

Reaction conditions: Cu-BTC MOF catalyst (0.050 g), oxidant (O₂ balloon), without solvent, 12 h at 80 °C.

ix). Effect of catalyst amount:

The effect of catalyst amount in the aerobic oxidation of benzylamine was studied using different amounts of catalyst viz., 10, 20, 30, 40, 50, 60 and 70 mg under identical conditions and the yields are found to be 20%, 50%, 79%, 90%, 98%, 98% and 99% respectively. This data shows

there is a significant influence on the yields upon increasing the amount of catalyst. The increase in the amount of catalyst from 10 to 50 mg indicated that an increase in the yields from 20 to 98% is observed. No significant changes either in the conversion or in the selectivity beyond a catalyst amount of 50 mg is observed. Based on these results it is concluded that an optimum catalyst load of 50 mg using a 7 mmol benzylamine produced maximum a yield of the desired compound.

Table S3: Effect of catalyst amount on the yield of the imine

S.No.	Substrate	Catalyst weight (mg)	Yield (%)
1	Benzylamine	10	20
2	Benzylamine	20	50
3	Benzylamine	30	79
4	Benzylamine	40	90
5	Benzylamine	50	98
6	Benzylamine	60	98
7	Benzylamine	70	99

Reaction conditions: Benzylamine (7 mmol), oxidant (O₂ balloon), without solvent, 12 h at 80 °C.

x). Effect of reaction time:

The experiments were performed at different time intervals (2, 6, 9, 12 and 16 h) over Cu-BTC MOF catalyst and the results are reported in Table 5, which showed that there is a gradual increase in the yield from 15 to 98% upon increasing the reaction time from 2 to 12 h. Within just 6 h, more than 50% of the desired product was detected. As the reaction proceeded with time, benzylamine was transformed into N-benzylbenzaldimine with 98% yield after 12 h. No significant change in reaction yield of the product with increase in reaction time from 12 to 16 h, implying that 12 h time is enough to convert the substrate with 100% selectivity towards the desired compound.

Table S4: Reaction time effect on the aerobic oxidation of benzylamine

S.No.	Substrate	Time (h)	Yield (%)
1	Benzylamine	2	15
2	Benzylamine	6	52
3	Benzylamine	9	87
4	Benzylamine	12	98
5	Benzylamine	16	97

Reaction conditions: Cu-BTC MOF catalyst (0.050 g), benzylamine (7 mmol), oxidant (O₂ balloon), without solvent at 80 °C.

xi). Large scale setup:

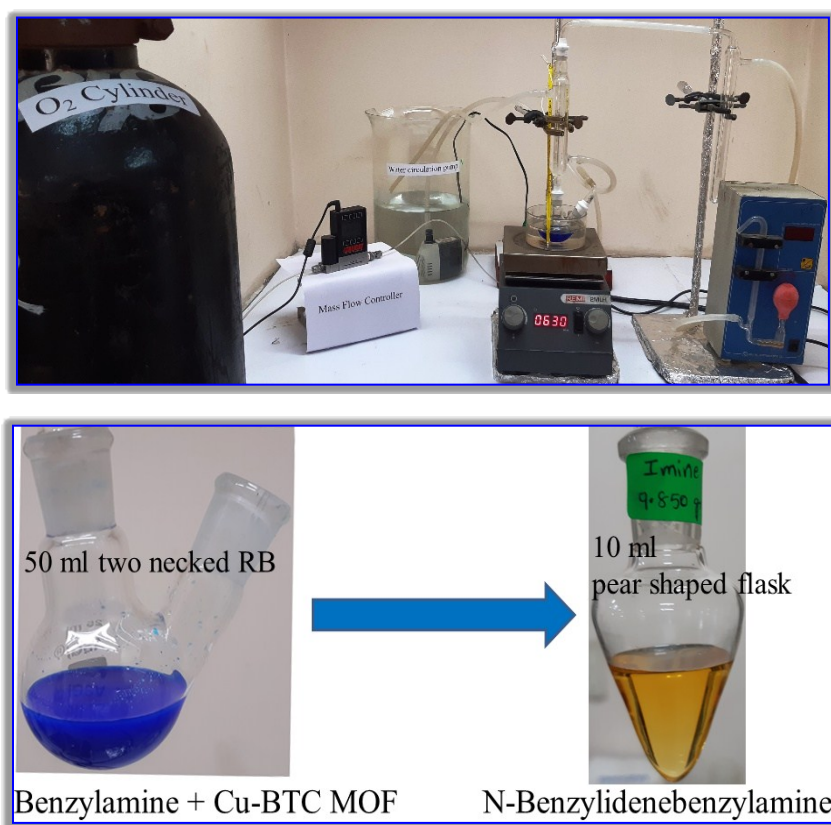


Fig. S6: Reaction apparatus for the 10 g scale operation.

xii). XRD analysis:

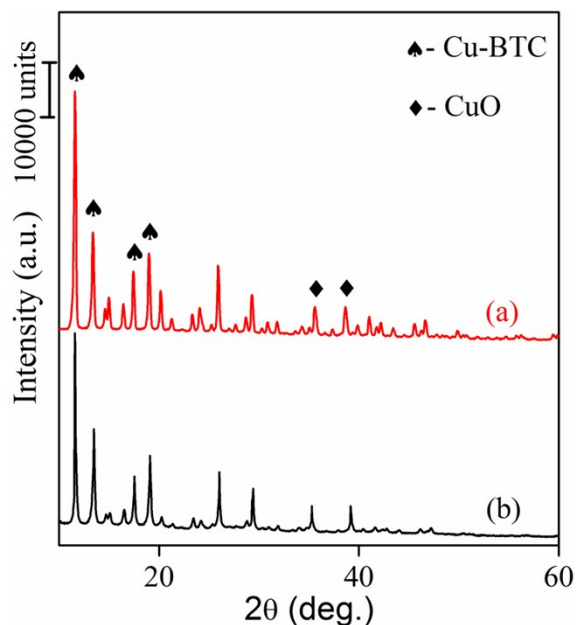


Fig. S7: Powder x-ray diffraction of (a) Cu-BTC MOF (fresh) and (b) Cu-BTC MOF (recovered after large scale operation) catalysts.

xiii). N₂ adsorption–desorption:

The N₂ adsorption-desorption isotherms of fresh and used Cu-BTC MOF catalysts were shown in Fig. S8. The data of the surface area pore volume and pore size are reported in Table S1. The fresh and used Cu-BTC MOF samples exhibit typical type IV isotherms with H4 hysteresis loops. The uptake of nitrogen in the P/P₀ range 0.4 to 1.0, which indicated a homogeneous pore size distribution⁹.

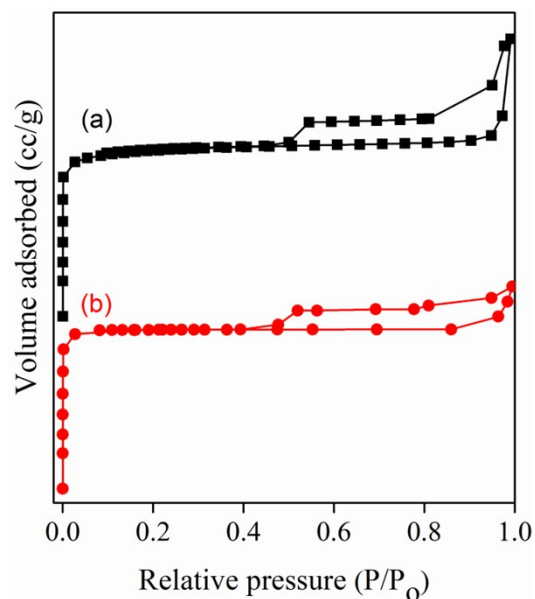


Fig. S8: N₂ adsorption–desorption (a) fresh and (b) used Cu-BTC MOF catalysts.

xiv). NH₃- temperature programmed desorption (TPD) analysis:

The TPD of NH₃ was carried out for Cu/SiO₂, Cu/TiO₂ and Cu/Al₂O₃ in order to measure the surface acidities of the catalysts. The TPD of NH₃ results indicated that the acid site densities are in the following order: Cu/SiO₂ < Cu/Al₂O₃ < Cu/TiO₂ (Table S5). Similarly, the catalytic activities followed the same trend in relation to the surface acidities measured by TPD of NH₃.

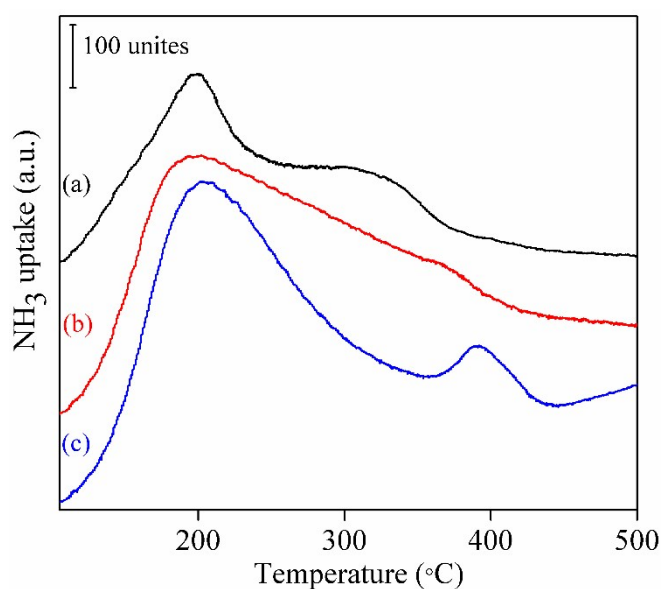


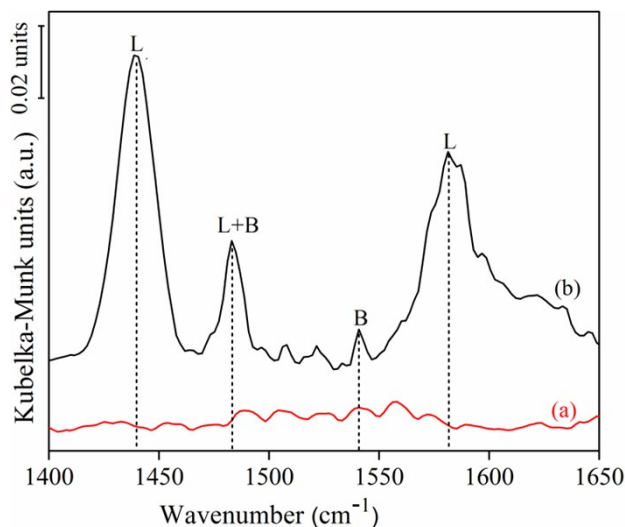
Fig. S9: TPD of NH₃ over 25wt%Cu supported on (a) TiO₂ (b) Al₂O₃ and (c) SiO₂ catalysts.

Table S5: Acid site distribution of supported Cu catalysts from NH₃-TPD analysis.

Catalyst	BET Surface area (m ² g ⁻¹)	mmol g _{cat} ⁻¹	μmol m ⁻²
25wt%Cu/TiO ₂	56	0.183	3.26
25wt%Cu/Al ₂ O ₃	210	0.311	1.48
25wt%Cu/SiO ₂	390	0.352	0.90

xv). Pyridine adsorbed DRIFT spectroscopy:

The TPD of NH₃ for the Cu-BTC MOF sample was not done as its stability is lower (<500 C). Hence pyridine IR studies were performed for this catalyst. The pyridine adsorbed pure BTC showed Brønsted acid sites. Quite contrast to this the Cu-BTC MOF catalyst exhibited both the Brønsted (1540 cm⁻¹) and Lewis acid sites (1445 cm⁻¹). From the normalized spectra it has been observed that a high proportion of Lewis acid sites are observed compared to the Brønsted acid sites present on the catalyst surface. A comparative analysis is also made in the manuscript (Fig. 4).

**Fig. S10:** Pyridine adsorbed DRIFT spectra of (a) BTC and (a) Cu-BTC MOF catalysts.

4. Spectral data of all products

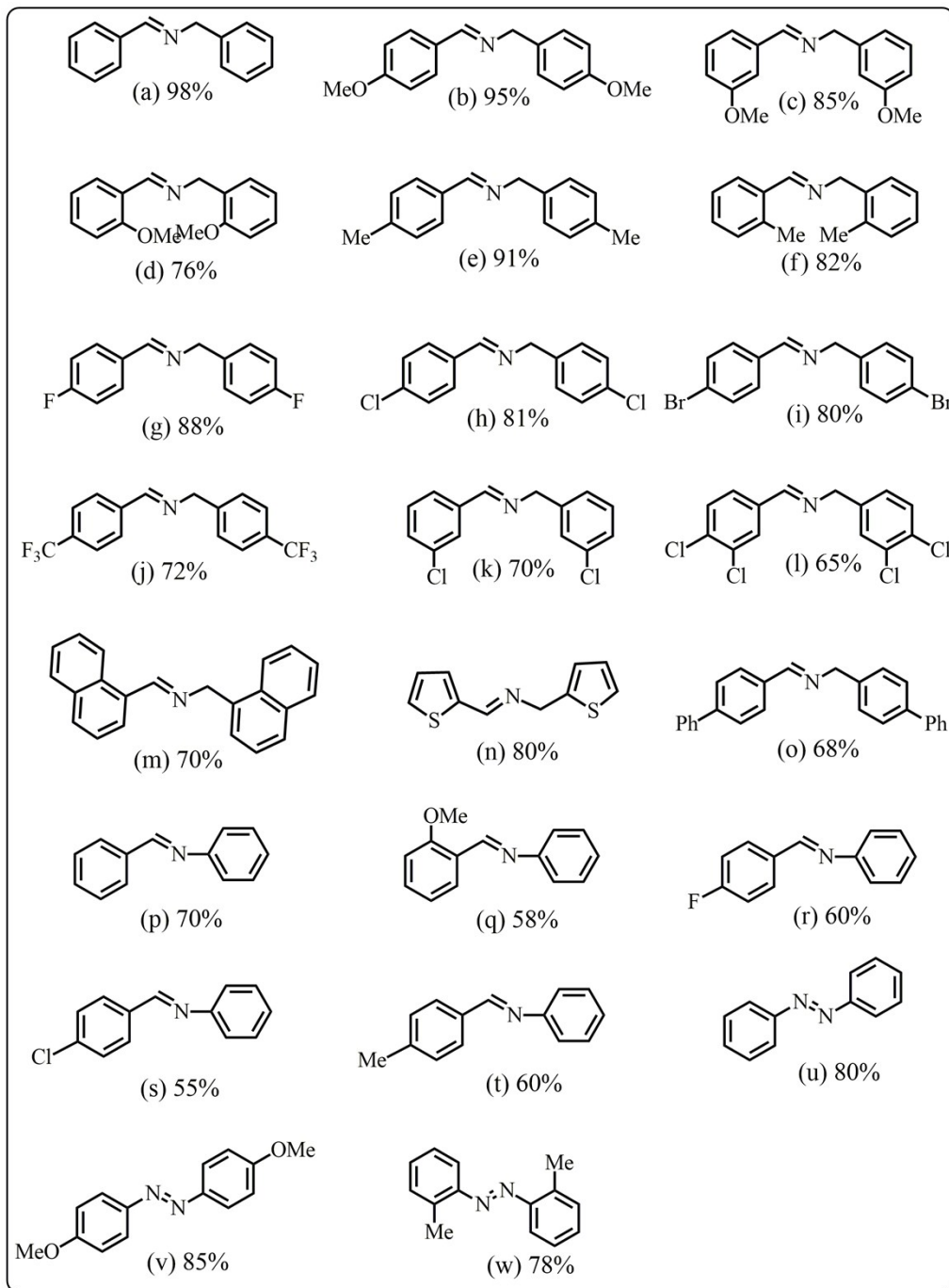
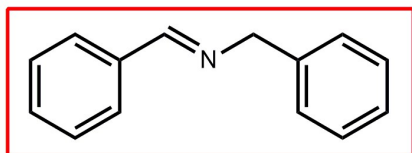


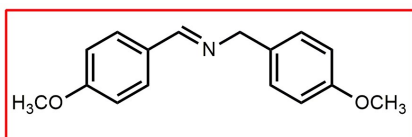
Fig. S11: Spectral data of imine products.

Spectral data:



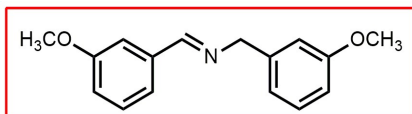
N-Benzylidenebenzylamine (Fig. S11a, 98% yield, yellow liquid)²;

¹H NMR (300MHz, CDCl₃): δ (ppm) = 8.36 (s, 1H), 7.78-7.75 (m, 2H), 7.40-7.19 (m, 8H), 4.80 (s, 2H); ¹³C NMR (100 MHz, CDCl₃): δ (ppm) = 161.83, 139.15, 136.01, 130.62, 128.45, 128.35, 128.14, 127.83, 126.84, 64.88.



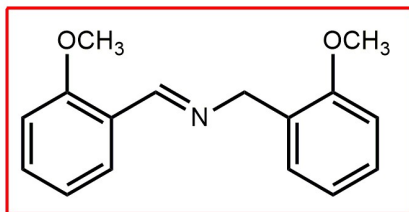
N-(4-Methoxybenzylidene)-4-methoxyphenylmethylamine (Fig. S11b, 95% yield, yellow liquid)²;

¹H NMR (300MHz, CDCl₃): δ (ppm) = 8.20 (s, 1H), 7.7-7.6 (d, J = 8.5 Hz, 2H), 7.23-7.20 (d, J = 8.4 Hz, 2H), 6.90-6.83 (m, 4H), 4.68 (s, 2H), 3.76 (s, 3H), 3.73 (s, 3H). ¹³C NMR (125 MHz, CDCl₃): δ (ppm) = 161.5, 160.8, 158.47, 131.47, 129.65, 129.0, 113.8, 113.72, 64.19, 55.15, 55.08.



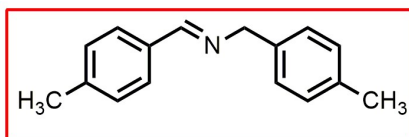
N-(3-Methoxybenzylidene)-3-methoxyphenylmethylamine (Fig. S11c, 85% yield, yellow liquid)³;

¹H NMR (500MHz, CDCl₃): δ (ppm) = 8.31 (s, 1H), 7.38-7.37 (m, 1H), 7.31-7.21 (m, 3H), 6.97-6.94 (m, 1H), 6.91-6.89 (m, 2H), 6.80-6.77 (dd, J = 8.0, 2.5 Hz, 1H), 4.76 (s, 2H), 3.79 (s, 3H), 3.76 (s, 3H). ¹³C NMR (100 MHz, CDCl₃): δ (ppm) = 161.9, 159.75, 159.64, 140.67, 137.42, 129.43, 129.35, 121.50, 120.18, 117.41, 113.51, 112.29, 111.55, 64.72, 55.21, 55.04.



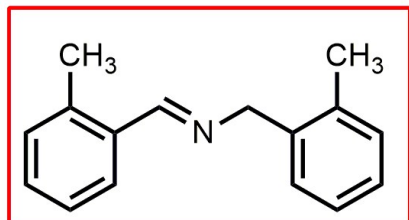
***N*-(2-Methoxybenzylidene)-2-methoxyphenylmethylamine** (Fig. S11d, 76% yield, yellow liquid)²;

¹H NMR (400 MHz, CDCl₃): δ (ppm) = 8.83 (s, 1H), 8.03-8.01 (d, J = 7.7 Hz, 1H), 7.34-7.15 (m, 3H), 6.95-6.80 (m, 4H), 4.81 (s, 2H), 3.78 (s, 6H). ¹³C NMR (125.4 MHz, CDCl₃): δ (ppm) = 158.51, 158.09, 156.79, 131.58, 128.8, 127.80, 127.70, 127.18, 124.53, 120.46, 120.25, 110.75, 109.94, 59.38, 55.23, 55.06.



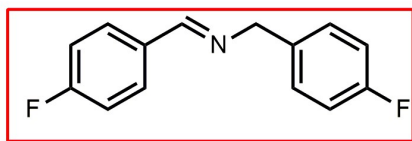
***N*-(4-Methylbenzylidene)-4-methylphenylmethylamine** (Fig. S11e, 91% yield, White solid)³;

¹H NMR (500 MHz CDCl₃): δ (ppm) = 8.33 (s, 1H), 7.66-7.65 (d, J = 8.08 Hz, 2H), 7.22-7.19 (m, 4H), 7.147.13 (d, J = 7.78 Hz, 2H), 4.76 (s, 2H), 2.37 (s, 3H), 2.33 (s, 3H). ¹³C NMR (100 MHz, CDCl₃): δ (ppm) = 161.64, 140.92, 136.45, 136.31, 133.58, 129.24, 129.10, 128.19, 127.91, 64.75, 21.46, 21.06.

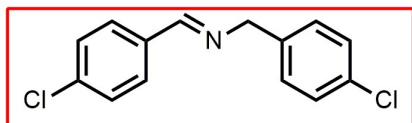


***N*-(2-Methylbenzylidene)-2-methylphenylmethylamine** (Fig. S11f, 82% yield, yellow liquid)³;

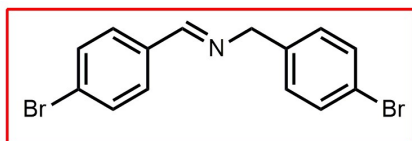
¹H NMR (300 MHz, CDCl₃): δ (ppm) = 8.64 (s, 1H), 7.93-7.90 (d, J = 7.5 Hz, 1H), 7.30-7.14 (m, 7H), 4.80 (s, 2H), 2.48 (s, 3H), 2.37 (s, 3H). ¹³C NMR (125 MHz, CDCl₃): δ (ppm) = 160.46, 137.62, 137.52, 136.0, 134.14, 130.72, 130.15, 130.01, 128.19, 127.61, 126.95, 126.08, 125.98, 63.20, 19.30, 19.20.



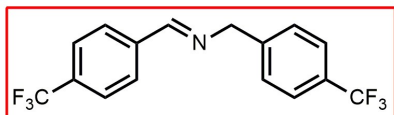
N-(4-Fluorobenzylidene)-4-fluorophenylmethanimine (Fig. S11g, 88% yield, yellow liquid)²;
¹H NMR (500 MHz, CDCl₃): δ (ppm) = 8.32 (s, 1H), 7.68-7.74 (m, 2H), 7.29-7.26 (m, 2H), 7.09-6.99 (m, 4H), 4.74 (s, 2H). ¹³C NMR (125.4 MHz, CDCl₃): δ (ppm) = 165, 163.0 (d, *J*_{C-F} = 243.0 Hz), 160.5, 134.7 (d, *J*_{C-F} = 2.2 Hz), 132.0 (d, *J*_{C-F} = 9.5 Hz), 130 (d, *J*_{C-F} = 8.8 Hz), 129.3 (d, *J*_{C-F} = 8.8 Hz), 115.5 (d, *J*_{C-F} = 22.0 Hz), 115.1 (d, *J*_{C-F} = 22.0 Hz), 64.2.



N-(4-Chlorobenzylidene)-4-chlorophenylmethanimine (Fig. S11h, 81% yield, white solid)²;
¹H NMR (300 MHz, CDCl₃): δ (ppm) = 8.32 (s, 1H), 7.71-7.68 (d, *J* = 8.49 Hz, 2H), 7.39-7.23 (m, 6H), 4.75 (s, 2H). ¹³C NMR (100 MHz, CDCl₃): δ (ppm) = 159.97, 139.06, 135.6, 135.09, 133.17, 130.68, 130.42, 129.75, 127.33, 63.50.

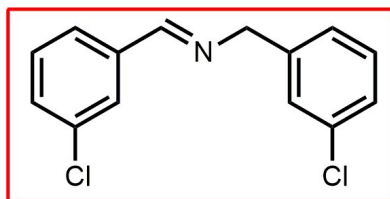


N-(4-bromobenzylidene)-1-(4-bromophenyl)methanimine (Fig. S11i, 80% yield)⁴;
¹H NMR (500 MHz, CDCl₃): δ (ppm) = 8.30 (s, 1H), 7.63-7.61 (m, 2H), 7.54-7.53 (m, 2H), 7.46-7.44 (m, 2H), 7.20-7.18 (d, *J* = 8.39 Hz, 2H), 4.72 (s, 2H). ¹³C NMR (125 MHz, CDCl₃): δ (ppm) = 160.83, 138.01, 134.77, 131.83, 131.53, 129.61, 129.57, 125.29, 120.86, 64.14.

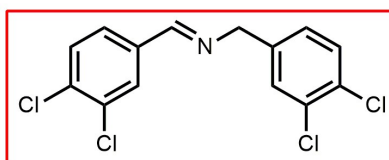


N-(4-(trifluoromethyl)benzylidene)-4-(trifluoromethyl)benzylamine (Fig. S11j, 72% yield)⁵;

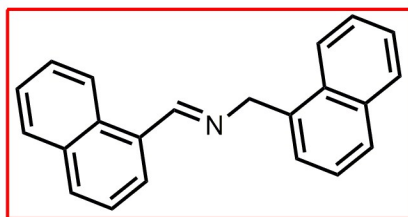
^1H NMR (500 MHz, CDCl_3): δ (ppm) = 8.42 (s, 1H), 7.88-7.87 (d, J = 8.08 Hz, 2H), 7.66-7.64 (d, J = 8.1 Hz, 2H), 7.59-7.58 (d, J = 8.1 Hz, 2H), 7.45-7.44 (d, J = 7.93 Hz, 2H), 4.86 (s, 2H). ^{13}C NMR (100 MHz, CDCl_3): δ (ppm) = 161.04, 143.02, 138.95, 132.61 (q, 32.5Hz), 129.6 (q, JC,F = 32.1 Hz), 128.4, 128.08, 125.56 (q, JC,F = 3.8 Hz), 125.39 (q, JC,F = 3.9Hz), 125.37 (q, JC,F = 270 Hz) 125.22 (q, J = 270 Hz), 64.28.



***N*-(3-Chlorobenzylidene)-3-chlorophenylmethanamine** (Fig. S11k, 70% yield, yellow liquid)²;
 ^1H NMR (400 MHz, CDCl_3): δ (ppm) = 8.30 (s, 1H), 7.79 (s, 1H), 7.61-7.59 (m, 1H), 7.39-7.19 (m, 6H), 4.75 (s, 2H). ^{13}C NMR (100 MHz, CDCl_3): δ (ppm) = 160.83, 140.95, 137.58, 134.76, 134.29, 130.81, 129.81, 129.70, 127.92, 127.85, 127.16, 126.50, 125.9, 64.16.

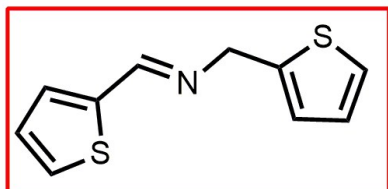


***N*-(3,4-dichlorobenzylidene)-1-(3,4-dichlorophenyl)methanamine** (Fig. S11l, 65% yield)⁴;
 ^1H NMR (300 MHz, CDCl_3): δ (ppm) = 8.30 (s, 1H), 7.88 (d, J = 2.6 Hz, 1H), 7.60-7.57 (dd, J = 8.3, 2.2 Hz, 1H), 7.51-7.48 (d, J = 8.3 Hz, 1H), 7.42-7.40 (d, J = 7.8 Hz, 2H), 7.18-7.15 (dd, J = 8.3, 2.1Hz, 1H), 4.74 (s, 2H). ^{13}C NMR (100 MHz, CDCl_3): δ (ppm) = 159.93, 139.05, 135.61, 135.00, 133.09, 132.44, 130.98, 130.62, 130.36, 129.67, 127.30, 127.13, 63.43.



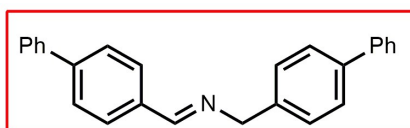
***N*-(1-naphthalenylmethylene)-1-naphthalenemethanamine** (Fig. S11m, 70% yield)²;

^1H NMR (400 MHz, CDCl_3): δ (ppm) = 9.03 (s, 1H), 8.93-8.91 (d, J = 8.4 Hz, 1H), 8.22-8.20 (d, J = 8.3 Hz, 1H), 7.90-7.77 (m, 5H), 7.56-7.42 (m, 7H), 5.36 (s, 2H); ^{13}C NMR (100 MHz, CDCl_3): δ (ppm) = 161.90, 135.41, 133.76, 133.71, 131.54, 131.25, 131.07, 129.16, 128.62, 128.53, 127.73, 127.12, 126.05, 125.96, 125.77, 125.63, 125.55, 125.14, 124.35, 123.87, 63.16.



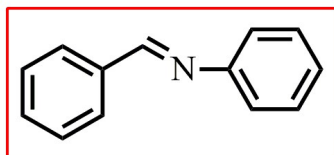
1-(thiophen-2-yl)-N-(thiophen-2-ylmethylene)ethanamine (Fig. S11n, 80% yield)⁵;

^1H NMR (500 MHz, CDCl_3): δ (ppm) = 8.41 (s, 1H), 7.41-7.40 (d, J = 5.03 Hz, 1H), 7.32-7.31 (d, J = 3.9 Hz, 1H), 7.23-7.22 (dd, J = 5.03, 3.6 Hz, 1H), 7.07-7.05 (m, 1H), 6.99-6.96 (m, 2H), 4.93 (s, 2H). ^{13}C NMR (100 MHz, CDCl_3): δ (ppm) = 155.37, 142.05, 141.46, 130.92, 129.29, 127.32, 126.82, 125.25, 124.78, 58.44.



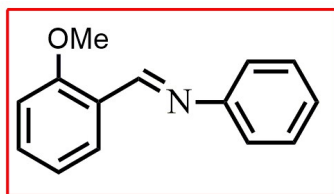
N-(1-biphenylmethylene)-1-biphenylethanamine (Fig. S11o, 68% yield)⁶;

^1H NMR (500 MHz, CDCl_3): δ (ppm) = 8.47 (s, 1H), 7.88-7.86 (d, J = 8.2 Hz, 2H), 7.67-7.58 (m, 8H), 7.47-7.32 (m, 8H), 4.89 (s, 2H). ^{13}C NMR (100 MHz, CDCl_3): δ (ppm) = 161.69, 143.52, 141.0, 140.37, 139.98, 138.36, 135.05, 128.83, 128.73, 128.40, 127.74, 127.30, 127.28, 127.13, 127.07, 64.82.



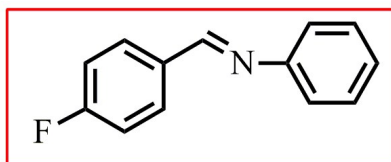
N-benzylideneaniline (Fig. S11p, 70% yield, brown oil)³;

^1H NMR (500 MHz, CDCl_3): δ (ppm) = 8.45 (s, 1H), 7.91-7.89 (m, 2H), 7.47-7.46 (m, 3H), 7.40-7.37 (m, 2H), 7.24-7.20 (m, 3H). ^{13}C NMR (100 MHz, CDCl_3): δ (ppm) = 160.37, 152.04, 136.17, 131.34, 129.11, 128.77, 128.73, 125.9, 120.8.



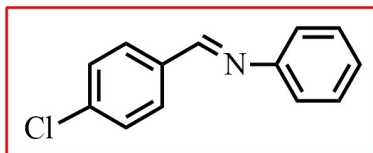
N-(2-methoxybenzylidene)aniline (Fig. S11q, 58% yield)⁸;

^1H NMR (400 MHz, CDCl_3): δ (ppm) = 8.91 (s, 1H), 8.16 – 8.13 (m, 1H), 7.45 – 7.35 (m, 3H), 7.25 – 7.18 (m, 3H), 7.05 – 7.01 (m, 1H), 6.98 – 6.95 (m, 1H), 3.88 (s, 3H), ^{13}C NMR (100 MHz, CDCl_3): δ (ppm) = 159.45, 156.48, 152.69, 132.63, 128.97, 127.47, 125.59, 121.01, 120.08, 111.05, 55.49.



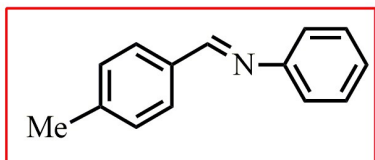
N-(4-Fluorobenzylidene)aniline (Fig. S11r, 60% yield, brown oil)³;

^1H NMR (400 MHz, CDCl_3): δ (ppm) = 8.42 (s, 1H), 7.92-7.89 (dd, J = 8.8, 5.6 Hz, 2H), 7.41-7.37 (m, 2H), 7.25-7.43 (m, 5H). ^{13}C NMR (100 MHz, CDCl_3): δ (ppm) = 165.8 (d, $J_{\text{C-F}}$ = 250.8 Hz), 158.8, 151.8, 132.6 (d, $J_{\text{C-F}}$ = 3.2 Hz), 130.8 (d, $J_{\text{C-F}}$ = 8.6 Hz), 129.2, 125.9, 120.7, 116.2 (d, $J_{\text{C-F}}$ = 22.3 Hz).



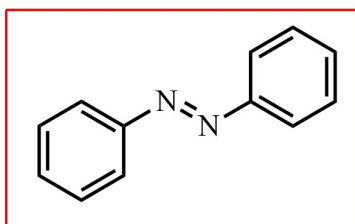
N-(4-Chlorobenzylidene)aniline (Fig. S11s, 55% yield, Orange solid)³;

^1H NMR (500 MHz, CDCl_3): δ (ppm) = 8.41 (s, 1H), 7.85 (d, J = 8.5 Hz, 2H), 7.45 (d, J = 8.4 Hz, 2H), 7.41-7.38 (m, 2H), 7.25-7.12 (m, 3H). ^{13}C NMR (100 MHz, CDCl_3): δ (ppm) = 158.8, 151.6, 137.34, 134.66, 130.8, 129.4, 129.04, 126.16, 120.81.



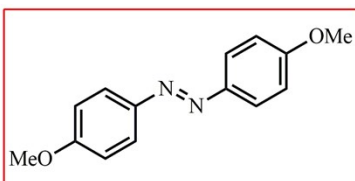
N-(4-Methylbenzylidene)aniline (Fig. S11t, 60% yield, brown oil)³;

¹H NMR (400 MHz, CDCl₃): δ (ppm) = 8.42 (s, 1H), 7.79 (d, J = 8.06 Hz, 2H), 7.40-7.36 (m, 2H), 7.28 (d, J = 8.0 Hz, 2H), 7.24-7.19 (m, 3H), 2.42 (s, 3H). ¹³C NMR (100 MHz, CDCl₃): δ (ppm) = 160.37, 153.1, 141.8, 133.64, 129.85, 129.5, 128.7, 125.72, 120.8, 21.8.



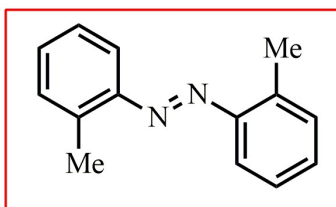
(E)-1,2-Diphenyldiazene (Fig. S11u, 80% yield)⁷;

¹H NMR (500 MHz, CDCl₃): δ (ppm) = 7.93-7.90 (m, 4H), 7.54-7.46 (m, 6H); ¹³C NMR (100 MHz, CDCl₃): δ (ppm) = 152.63, 130.96, 129.05, 122.82.



(E)-1,2-Bis(4-methoxyphenyl)diazene (Fig. S11v, 85% yield)⁷;

¹H NMR (400 MHz, CDCl₃): δ (ppm) = 7.88 (d, J = 9.0 Hz, 2H), 7.01 (d, J = 9.0 Hz, 4H), 3.88 (s, 6H); ¹³C NMR (100 MHz, CDCl₃): δ (ppm) = 161.52, 147.04, 124.30, 114.12, 55.57.



(E)-1,2-Di-o-tolyldiazene (Fig. S11w, 78% yield)⁷;

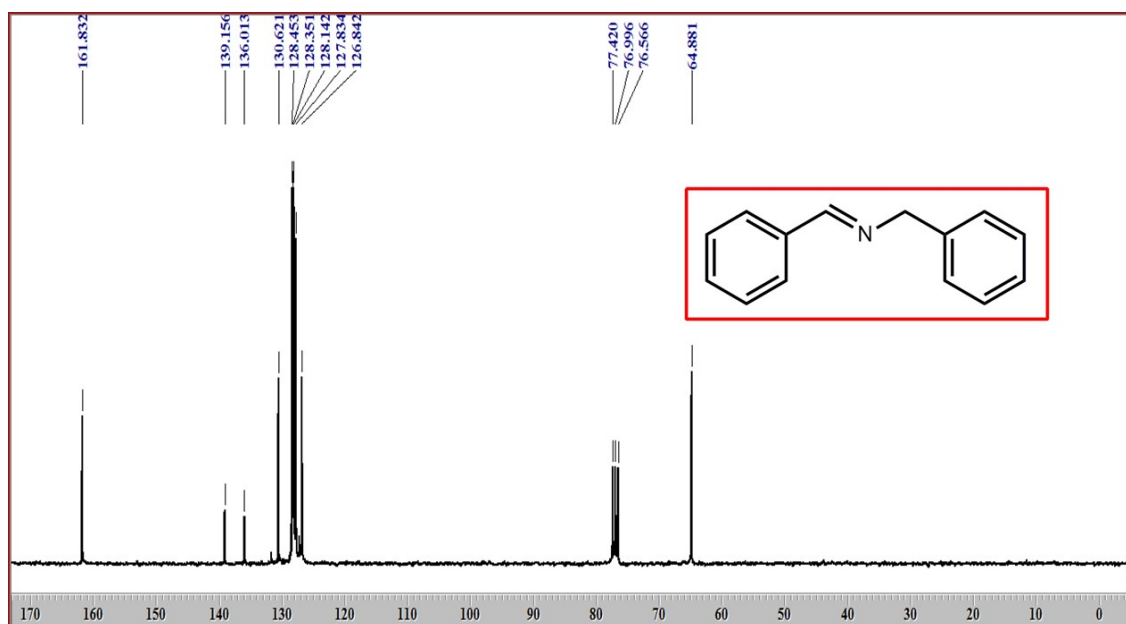
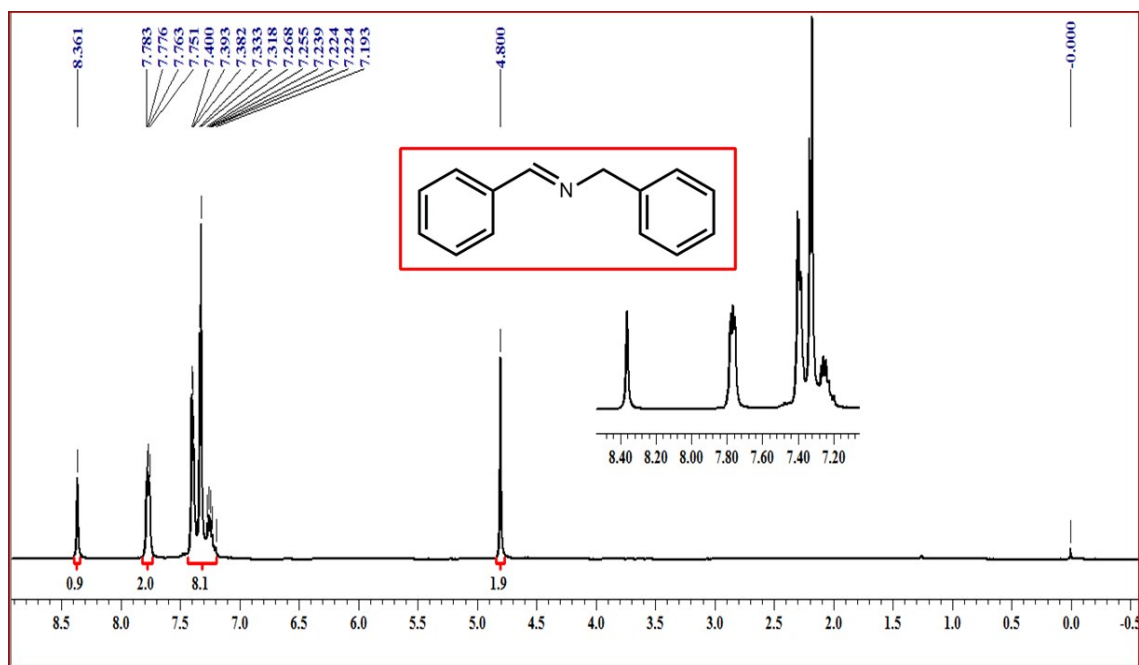
¹H NMR (400 MHz, CDCl₃): δ (ppm) = 7.66-7.63 (m, 2H), 7.34-7.30 (m, 4H), 7.26-7.24 (d, J = 8.0 Hz, 2H), 2.75 (s, 6H); ¹³C NMR (100 MHz, CDCl₃): δ (ppm) = 144.44, 130.27, 126.79, 122.13, 118.41, 114.76, 17.16.

References:

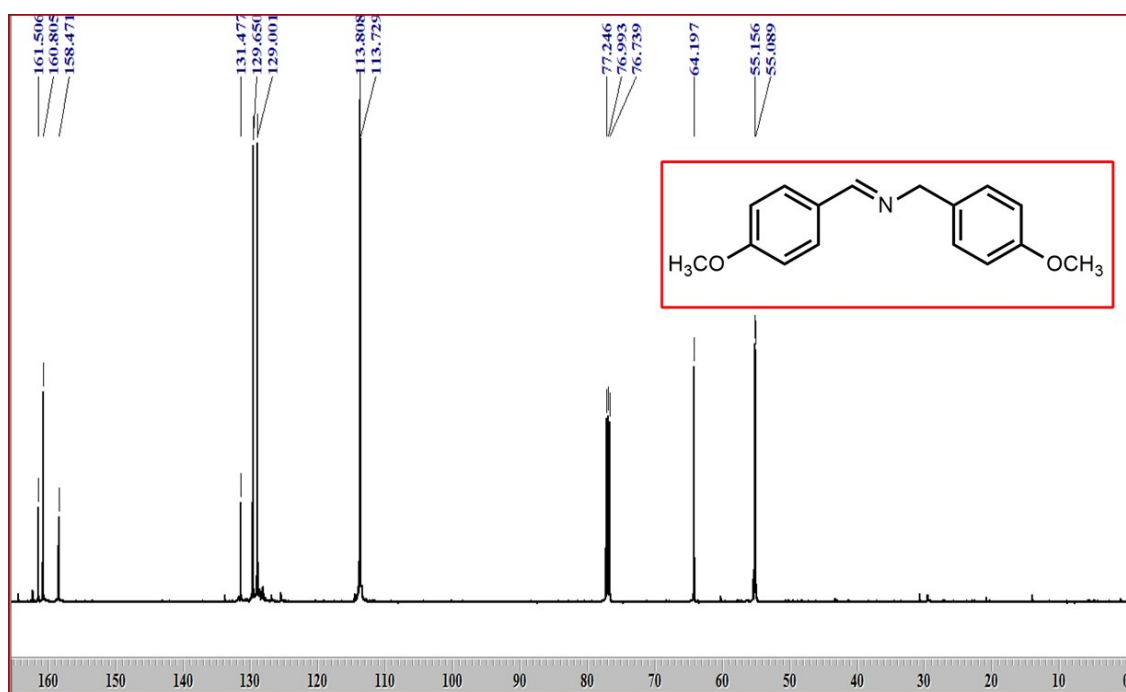
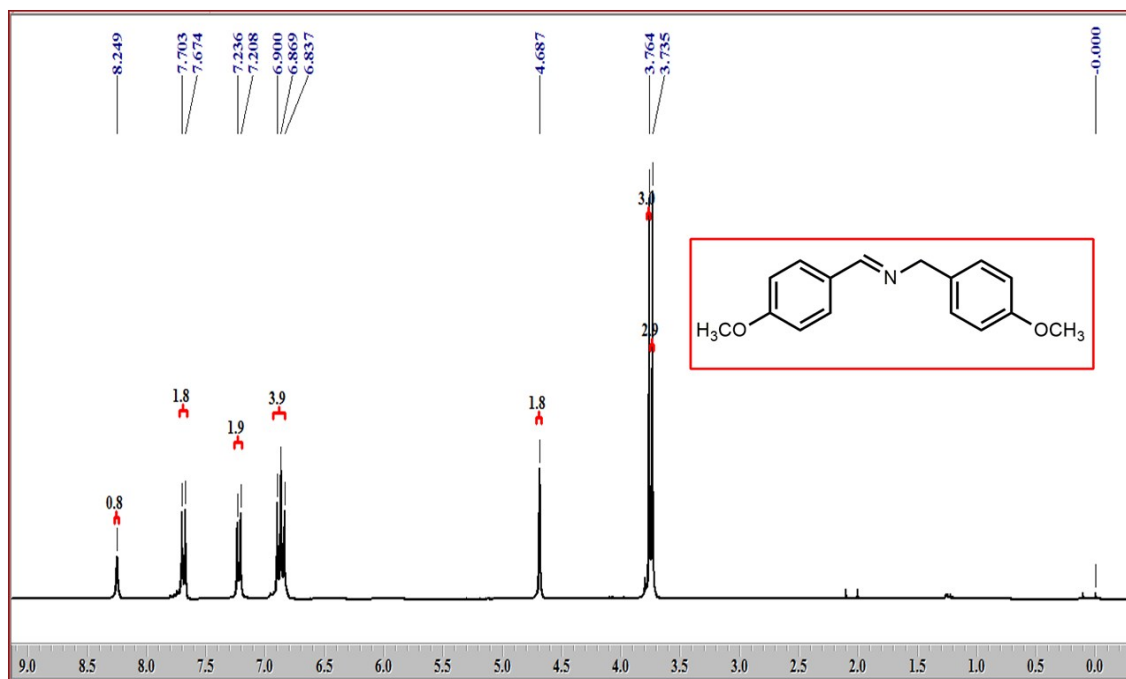
- 1 Y. Cheng, A. Kondo, H. Noguchi, H. Kajiro, K. Urita, T. Ohba, K. Kaneko and H. Kanoh, *Langmuir.*, 2009, **25**, 4510–4513.
- 2 A. E. Wendlandt and S. S. Stahl, *Org. Lett.*, 2012, **14**, 2850–2853
- 3 E. Zhang, H. Tian, S. Xu, X. Yu and Q. Xu, *Org. Lett.*, 2013, **15**, 2704–2707.
- 4 X. J. Yang, B. Chen, X. B. Li, L. Q. Zheng, L. Z. Wu and C. H. Tung, *Chem. Commun.*, 2014, **50**, 6664–6667.
- 5 S. Zhao, C. Liu, Y. Guo, J. C. Xiao and Q. Y. Chen, *J. Org. Chem.*, 2014, **79**, 8926–8931.
- 6 D. V. Jawale, E. Gravel, E. Villemin, N. Shah, V. Geertsen, I. N. N. Namboothiri and E. Doris, *Chem. Commun.*, 2014, **50**, 15251–15254.
- 7 Z. Hu and F. M. Kerton, *Org. Biomol. Chem.*, 2012, **10**, 1618–1624.
- 8 A.T. Murray, R. King, J. V. G. Donnelly, M. J. H. Dowley, F. Tuna, D. Sells, M. P. John and D. R. Carbery, *ChemCatChem*. **2016**, 8, 510–514.
- 9 A. Maleki, B. Hayati, M. Naghizadeh and S. W. Joo, *J Ind Eng Chem.*, 2015, **28**, 211-216.

^1H and ^{13}C NMR Spectra of products:

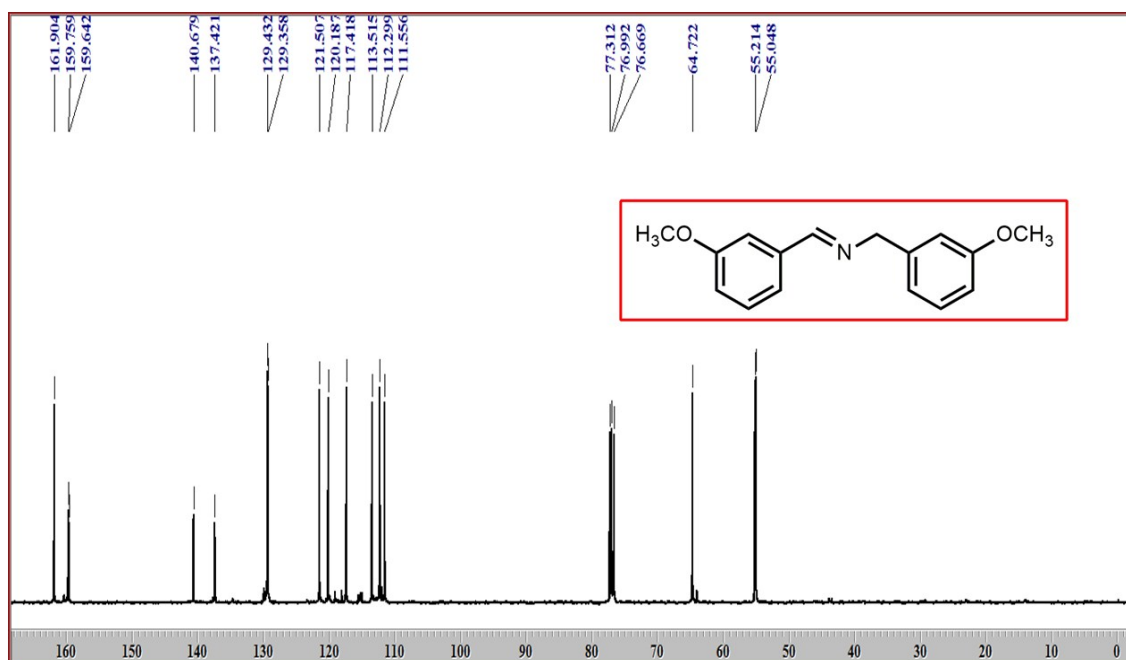
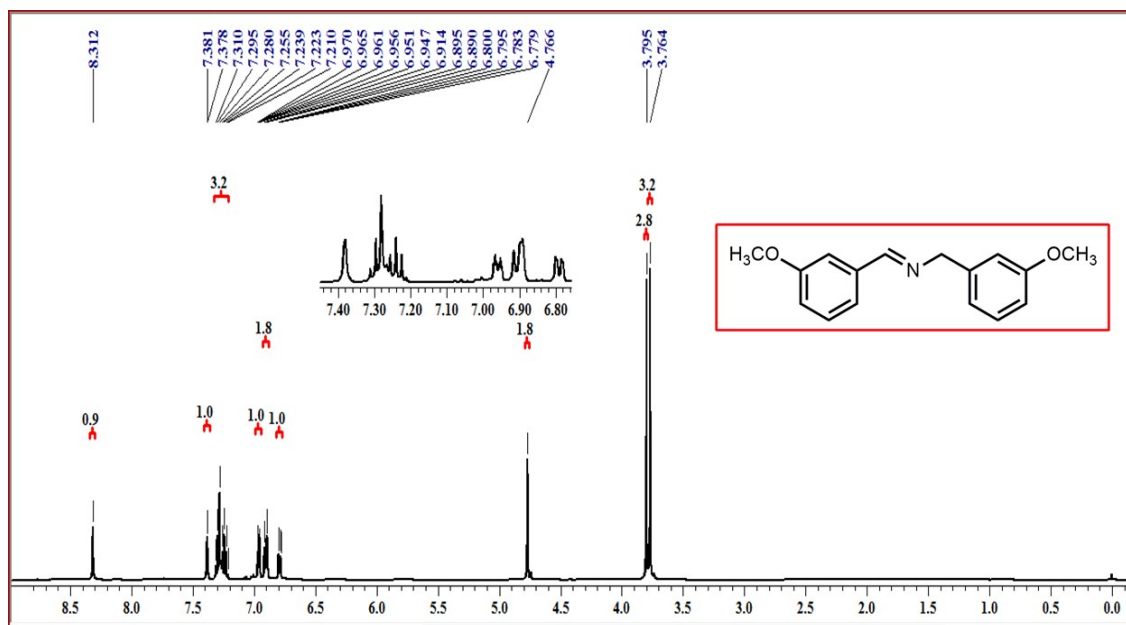
^1H and ^{13}C NMR Spectra of *N*-Benzylidenebenzylamine (Fig. S11a):



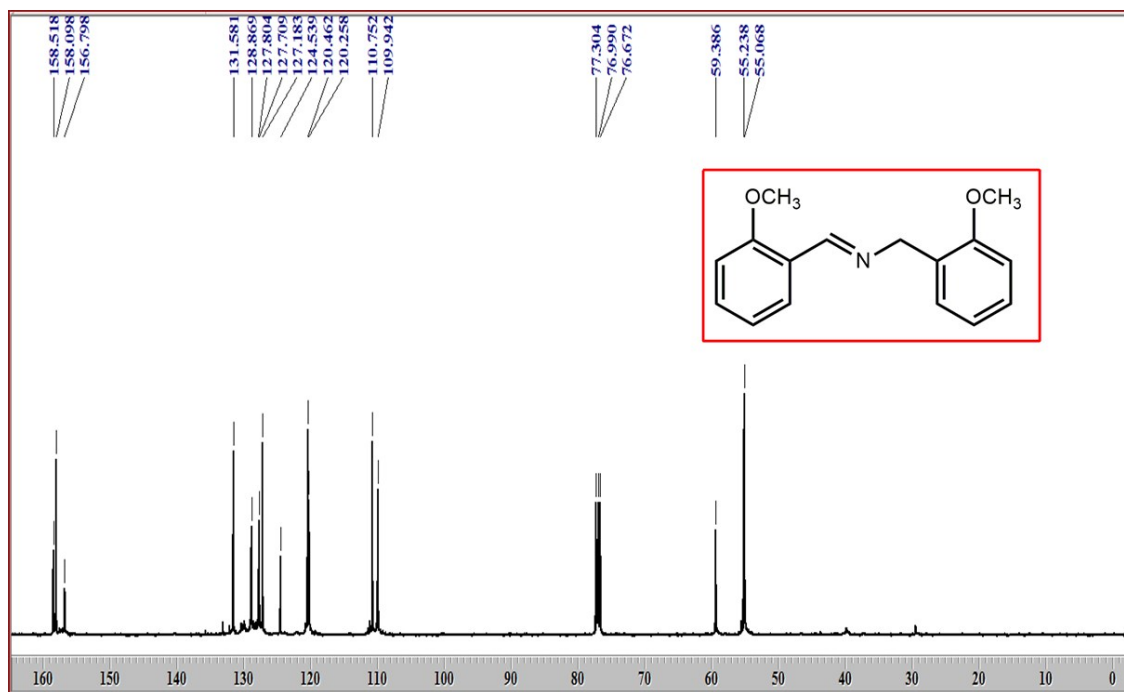
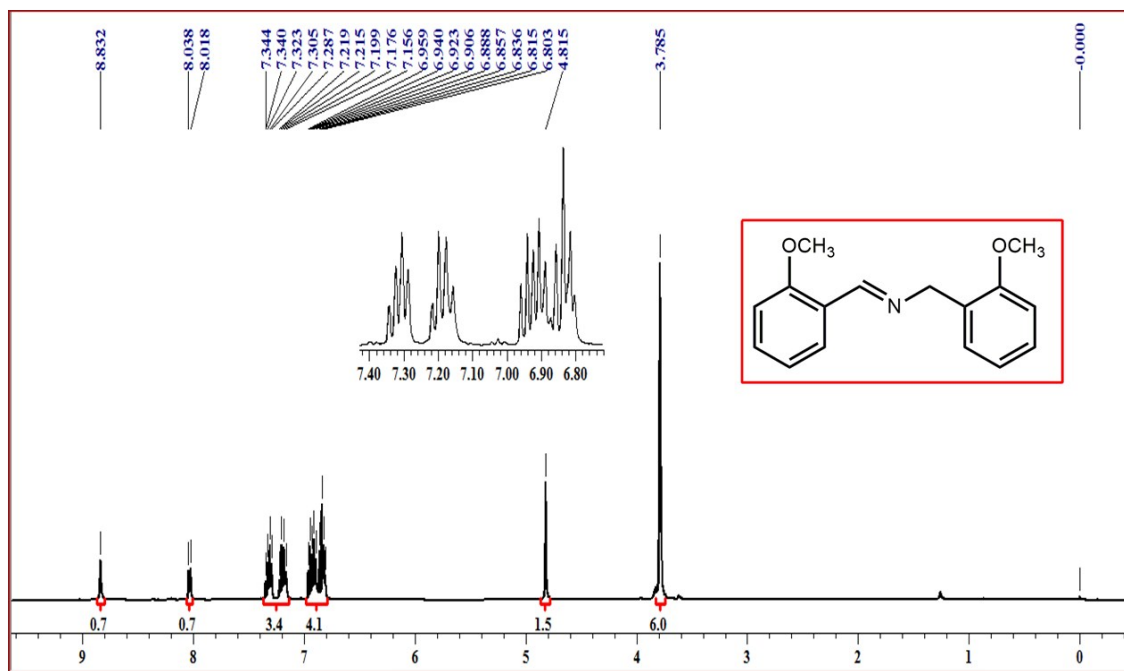
***N*-(4-Methoxybenzylidene)-4-methoxyphenylmethanamine (Fig. S11b):**



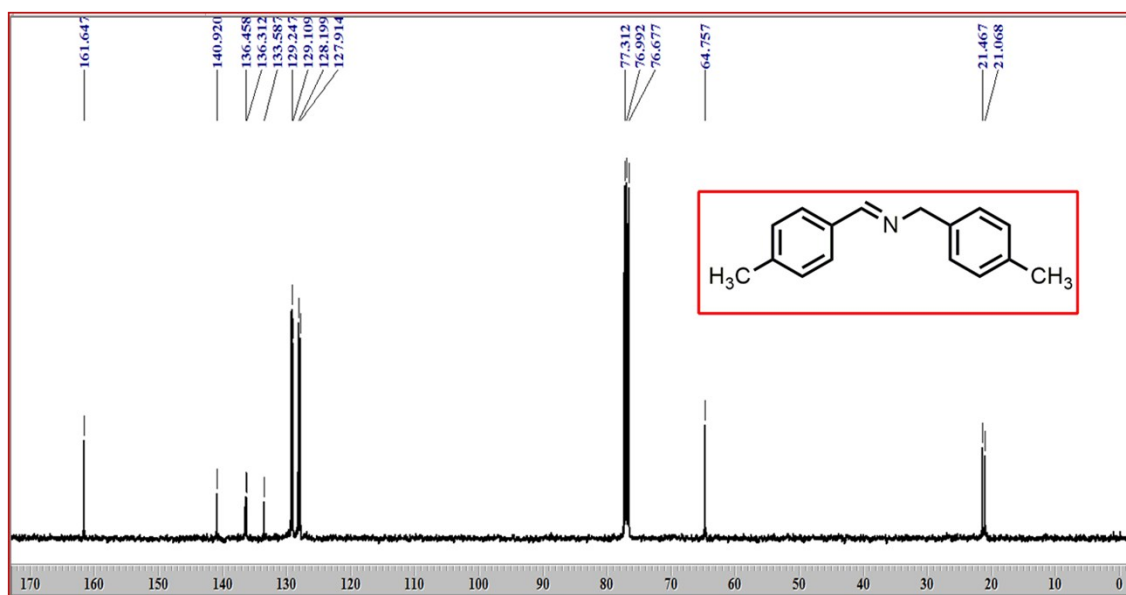
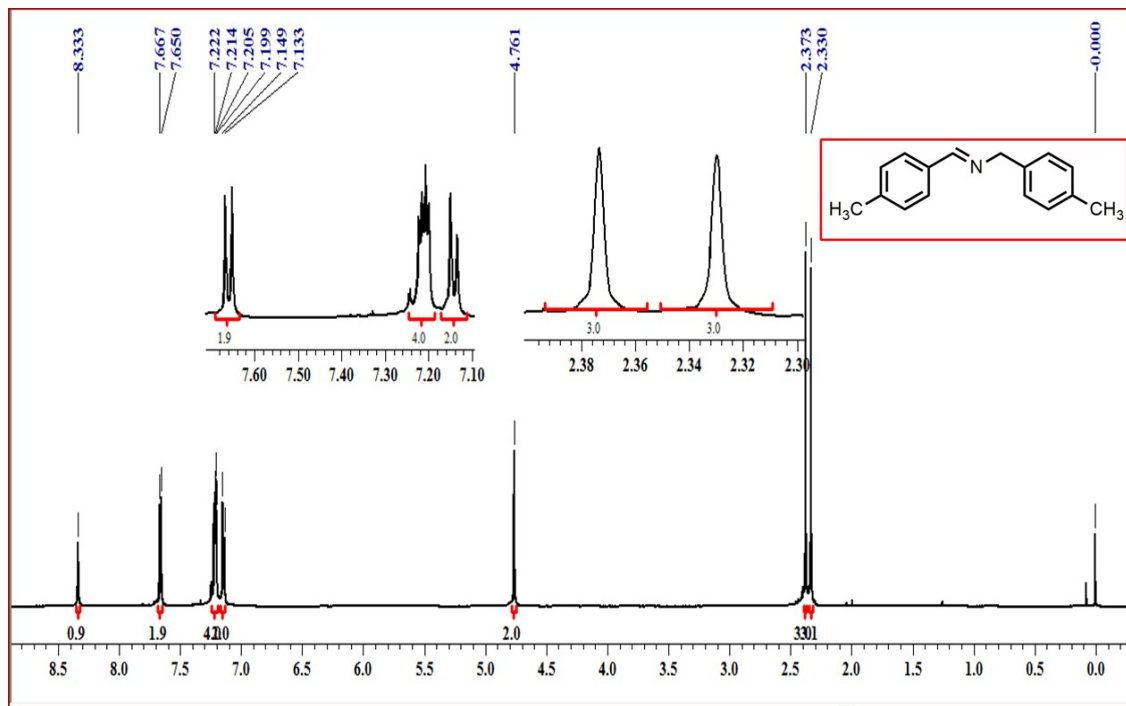
***N*-(3-Methoxybenzylidene)-3-methoxyphenylmethanamine (Fig. S11c):**



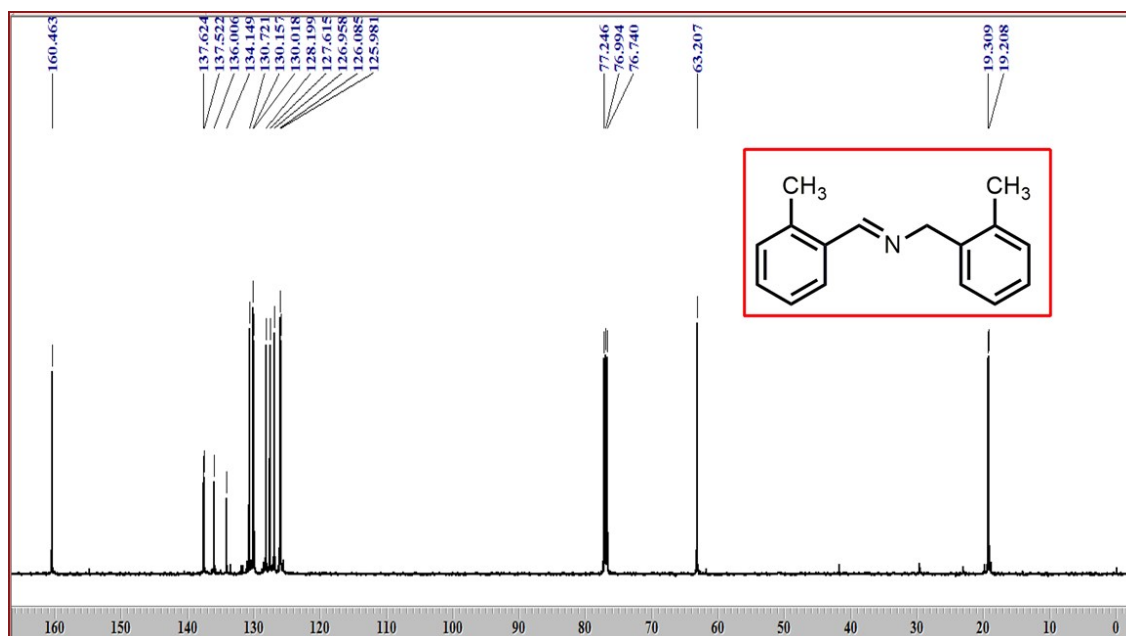
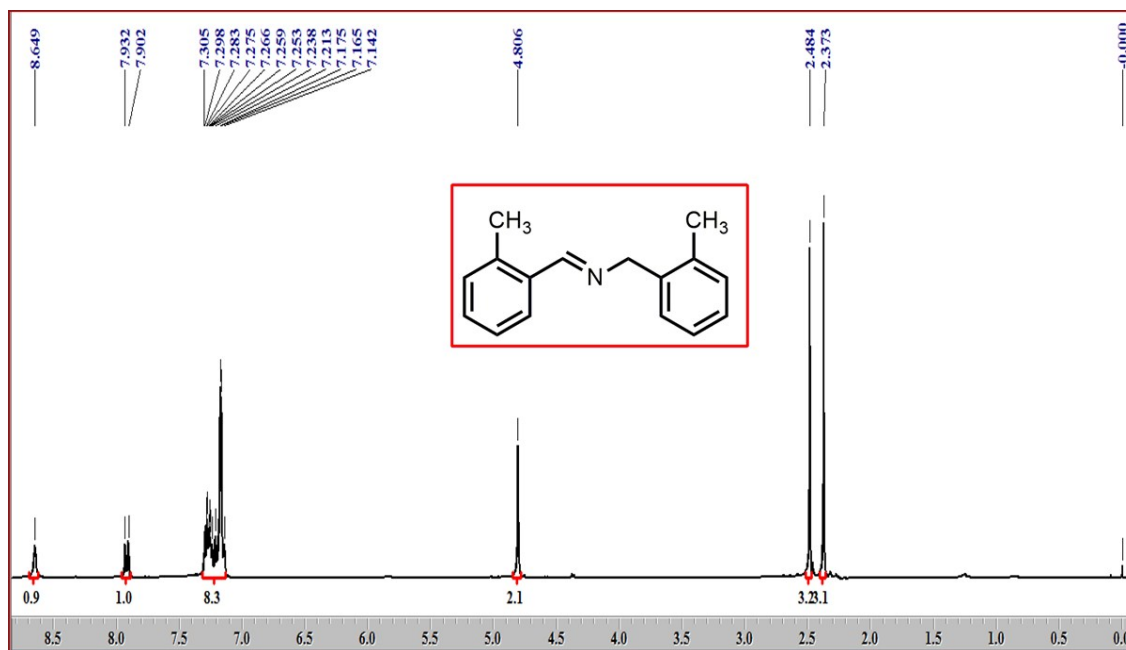
***N*-(2-Methoxybenzylidene)-2-methoxyphenylmethanamine (Fig. S11d):**



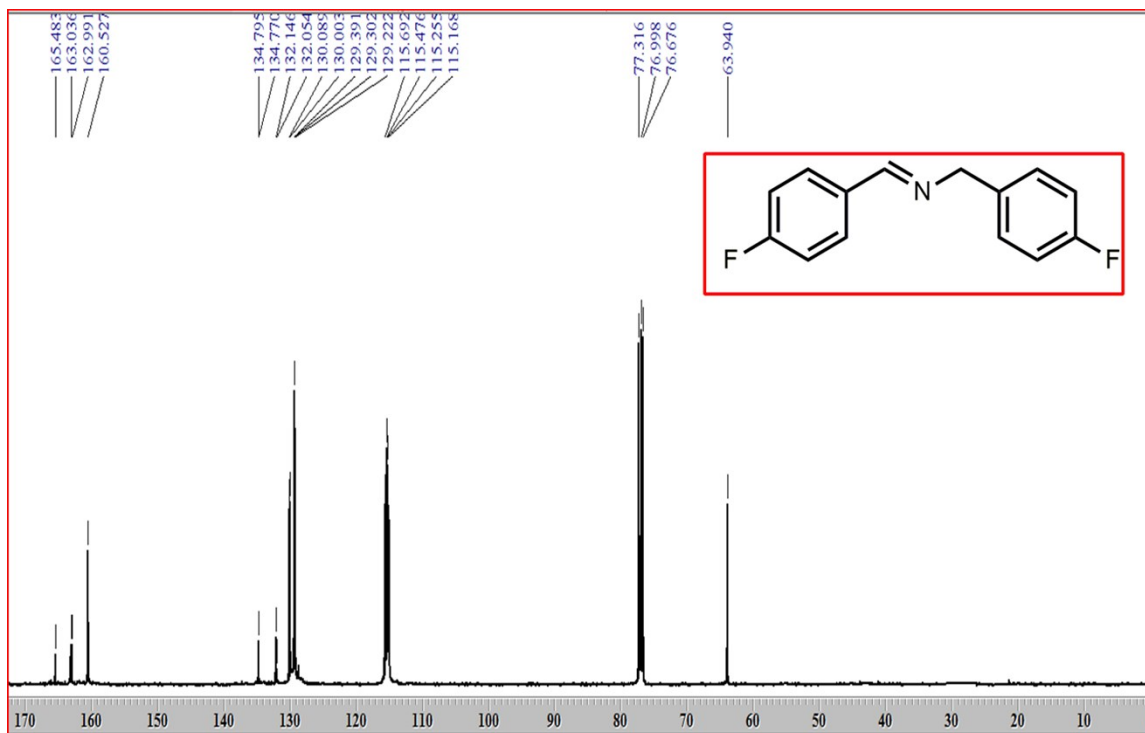
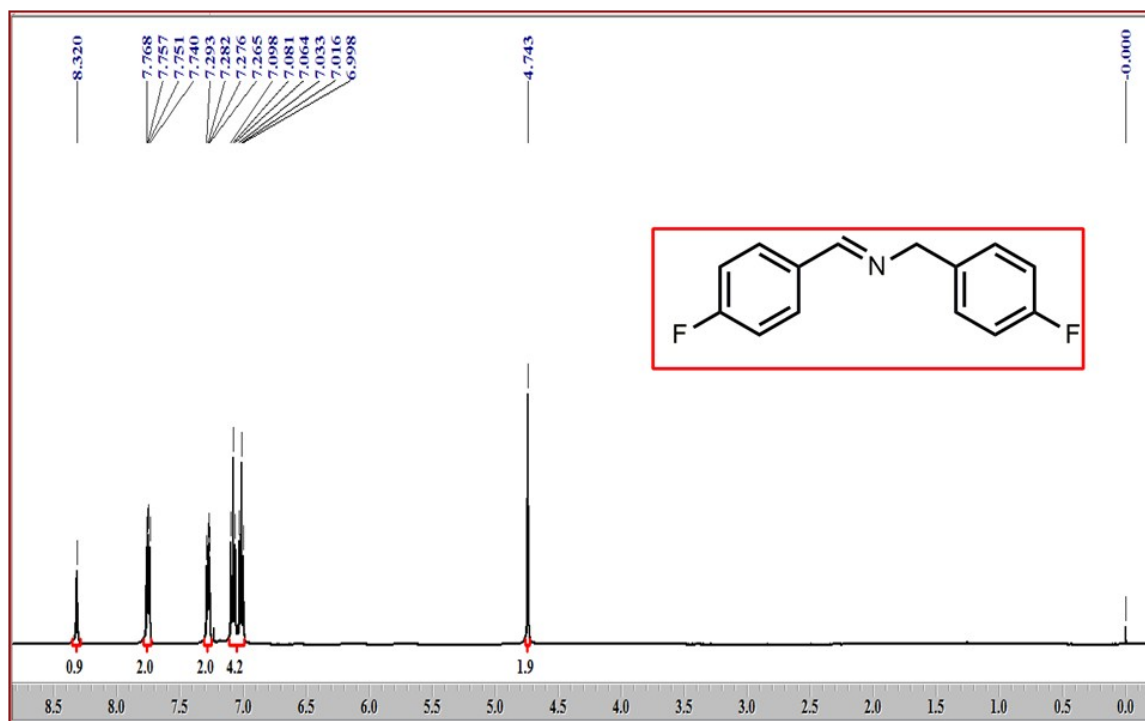
***N*-(4-Methylbenzylidene)-4-methylphenylmethylamine (Fig. S11e):**



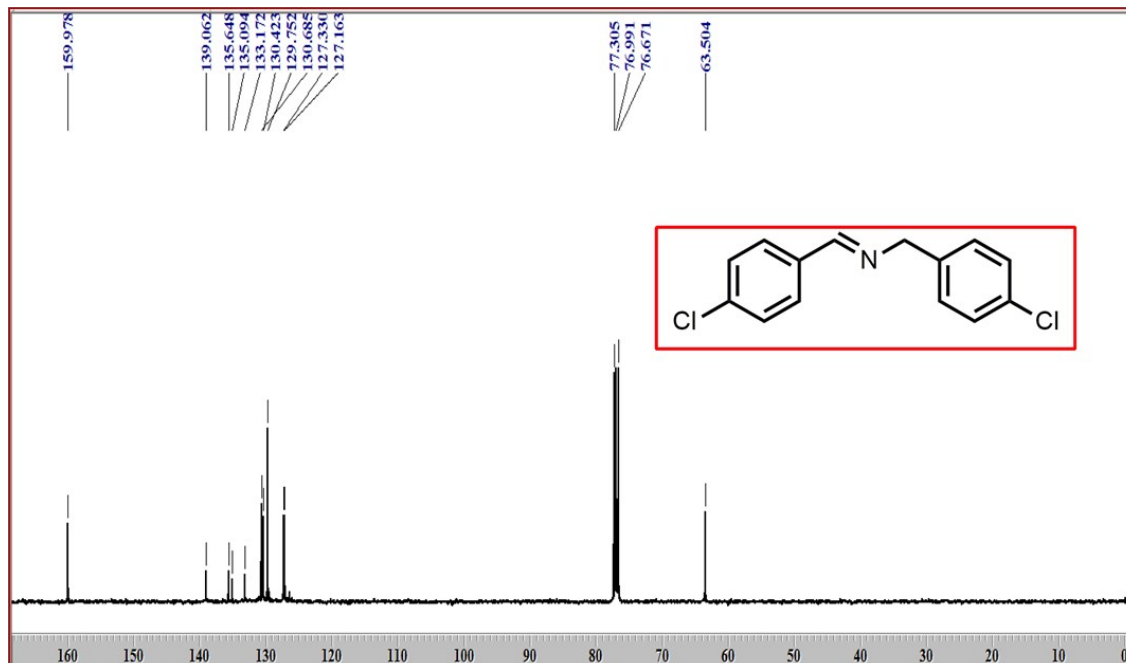
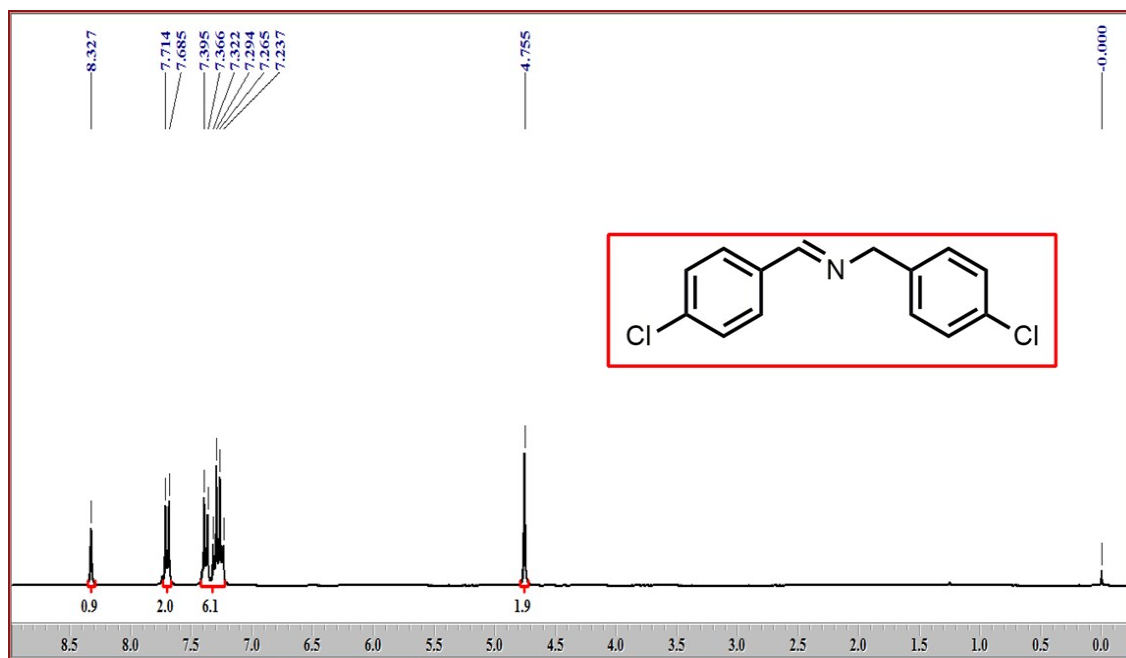
***N*-(2-Methylbenzylidene)-2-methylphenylmethanamine (Fig. S11f):**



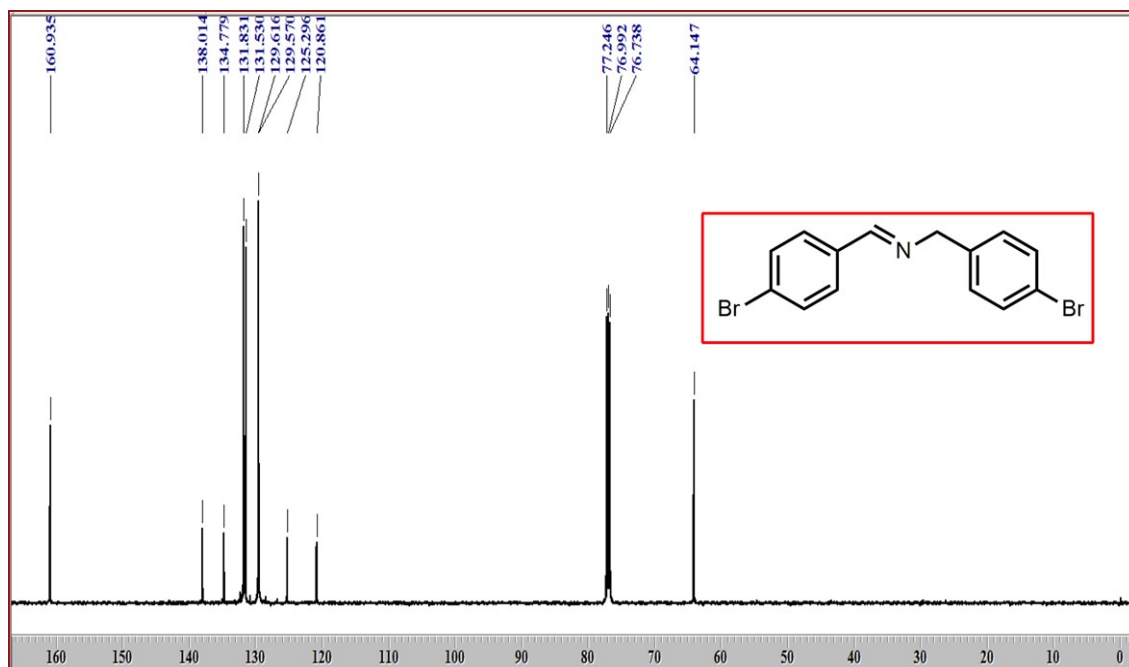
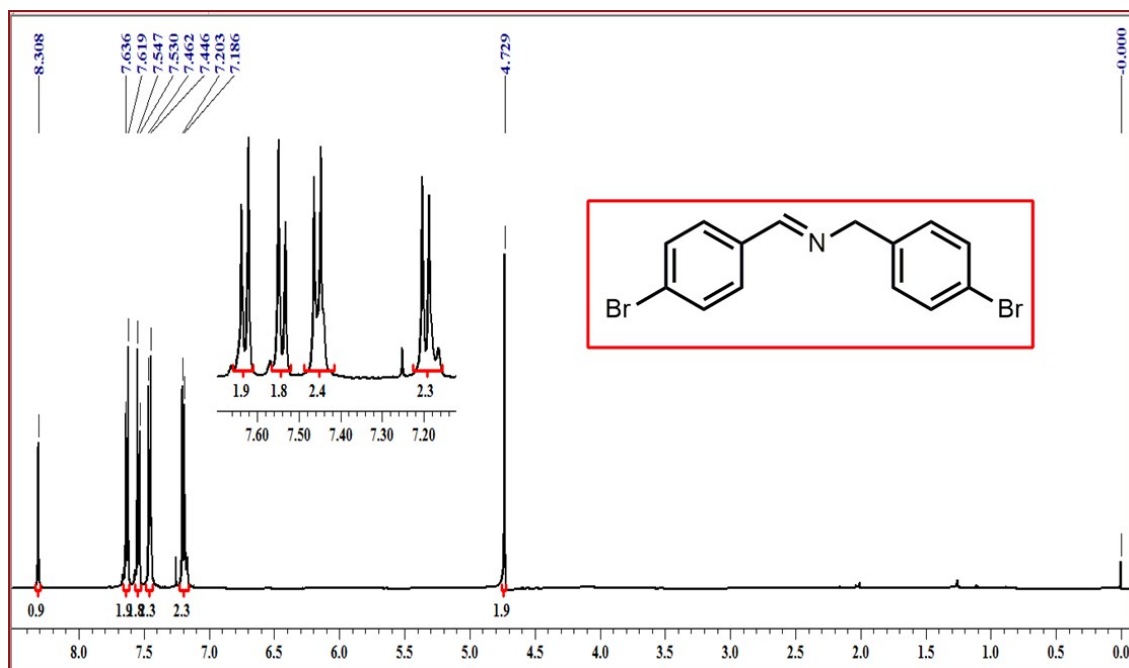
***N*-(4-Fluorobenzylidene)-4-fluorophenylmethanamine (Fig. S11g):**



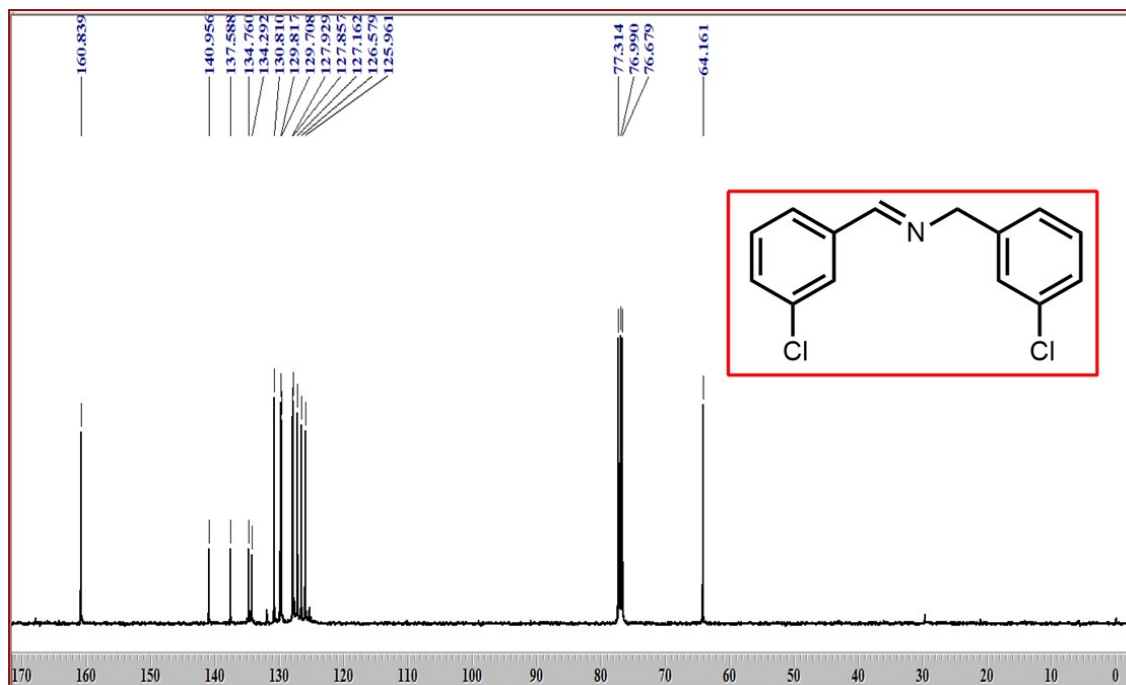
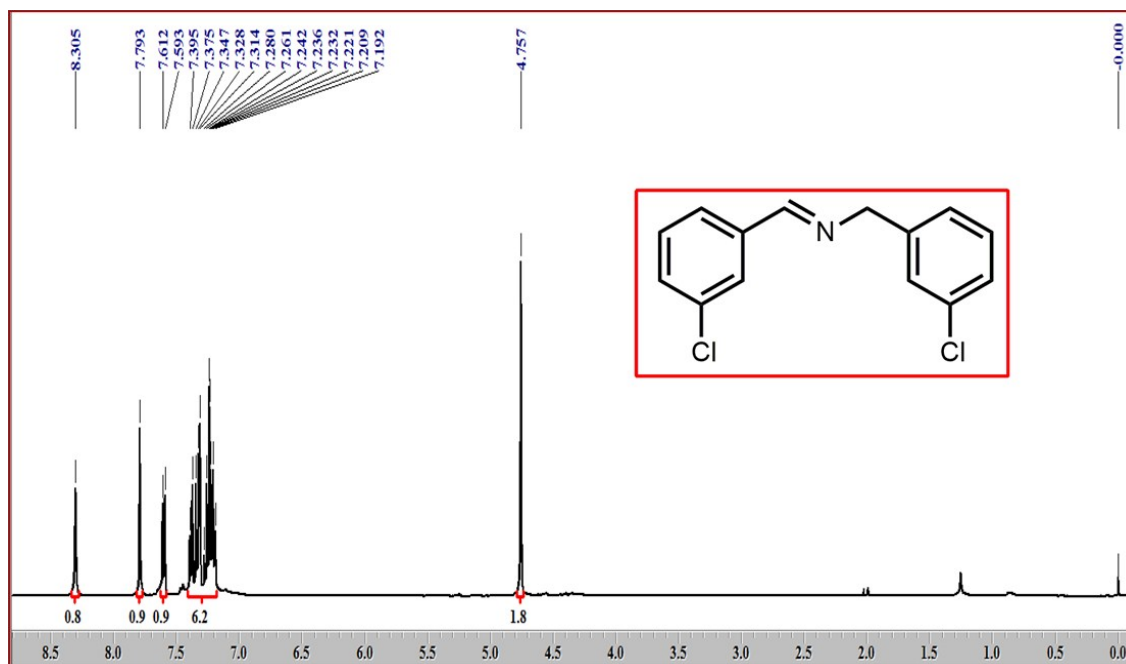
***N*-(4-Chlorobenzylidene)-4-chlorophenylmethanamine (Fig. S11h):**



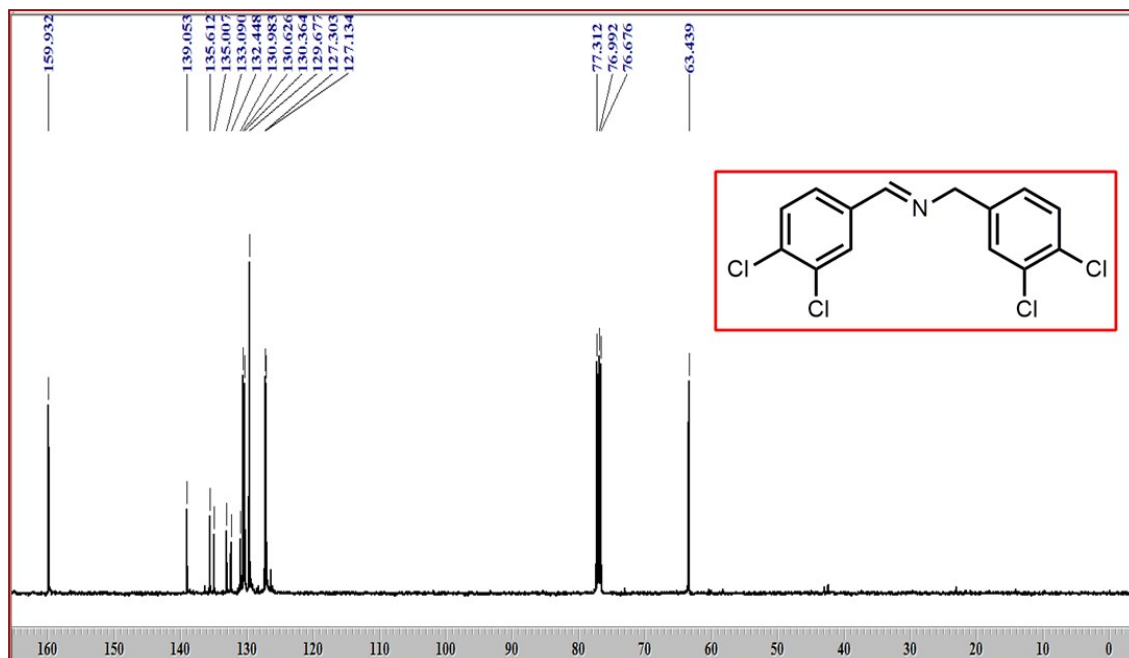
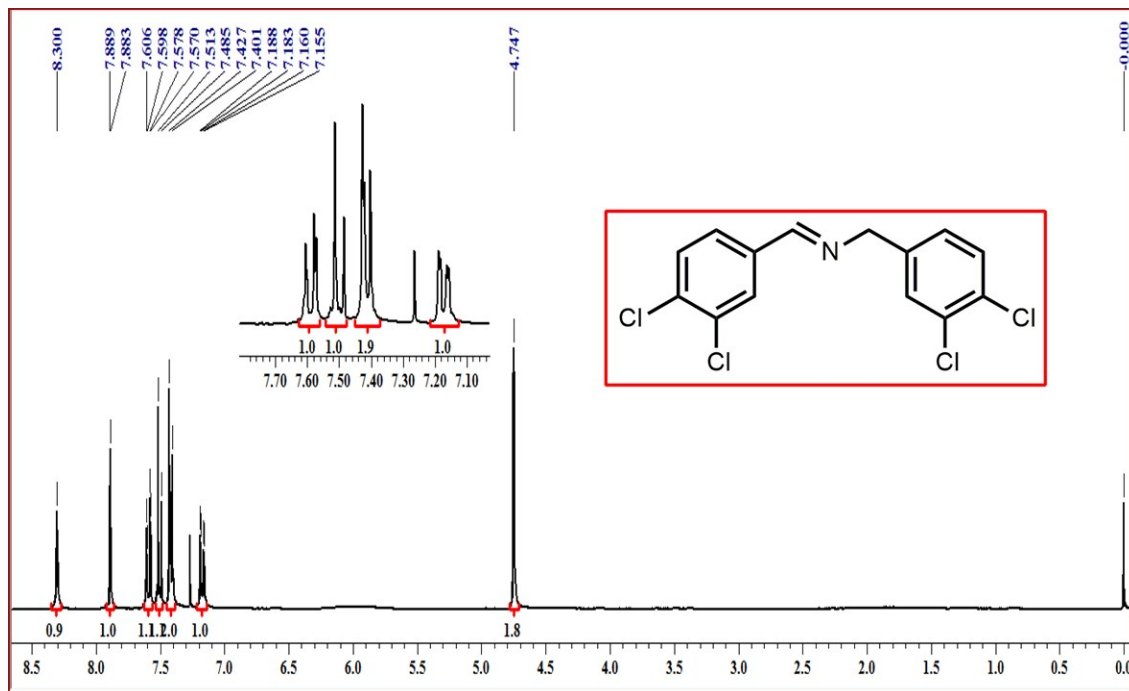
N-(4-bromobenzyliden)-1-(4-bromophenyl)methanamine (Fig. S11i):



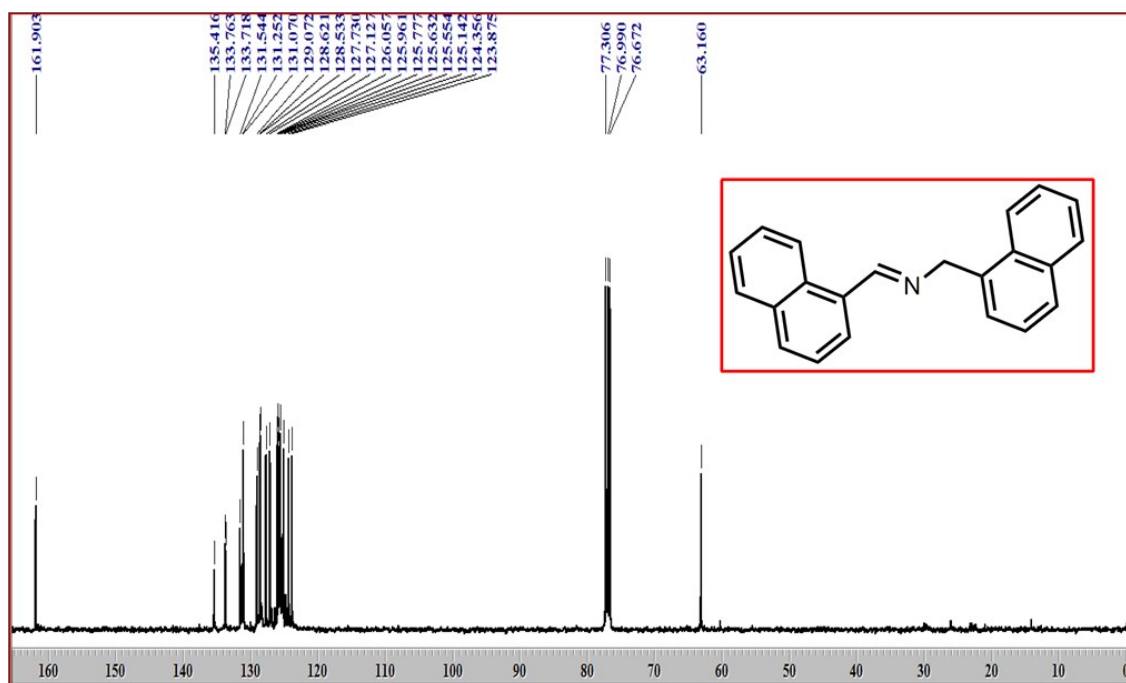
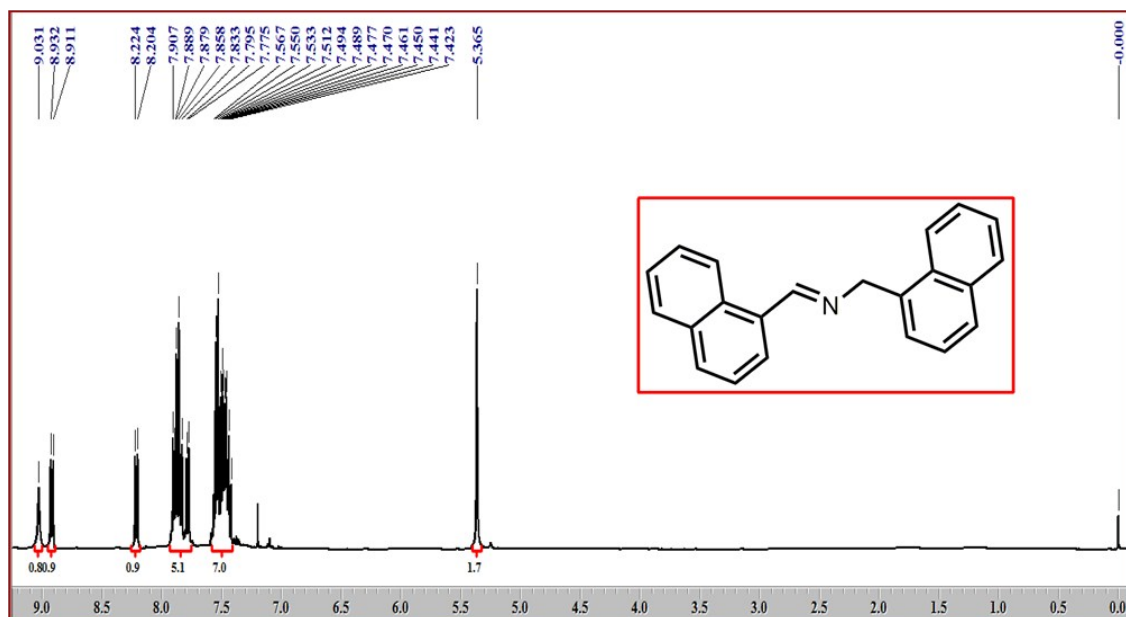
N-(3-Chlorobenzylidene)-3-chlorophenylmethanamine (Fig. S11k):



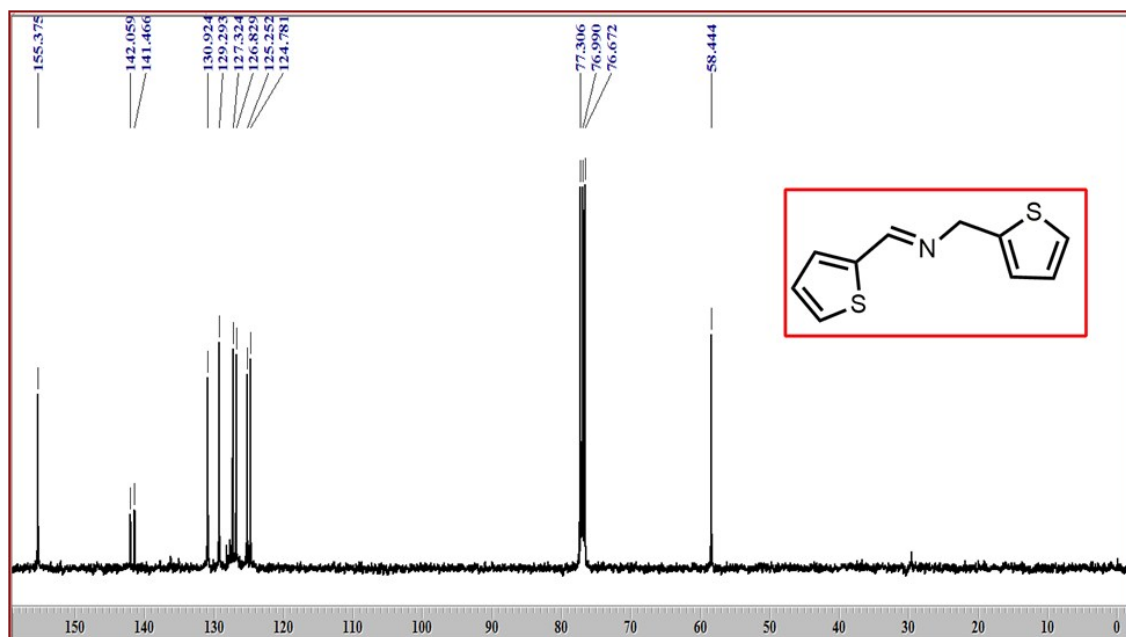
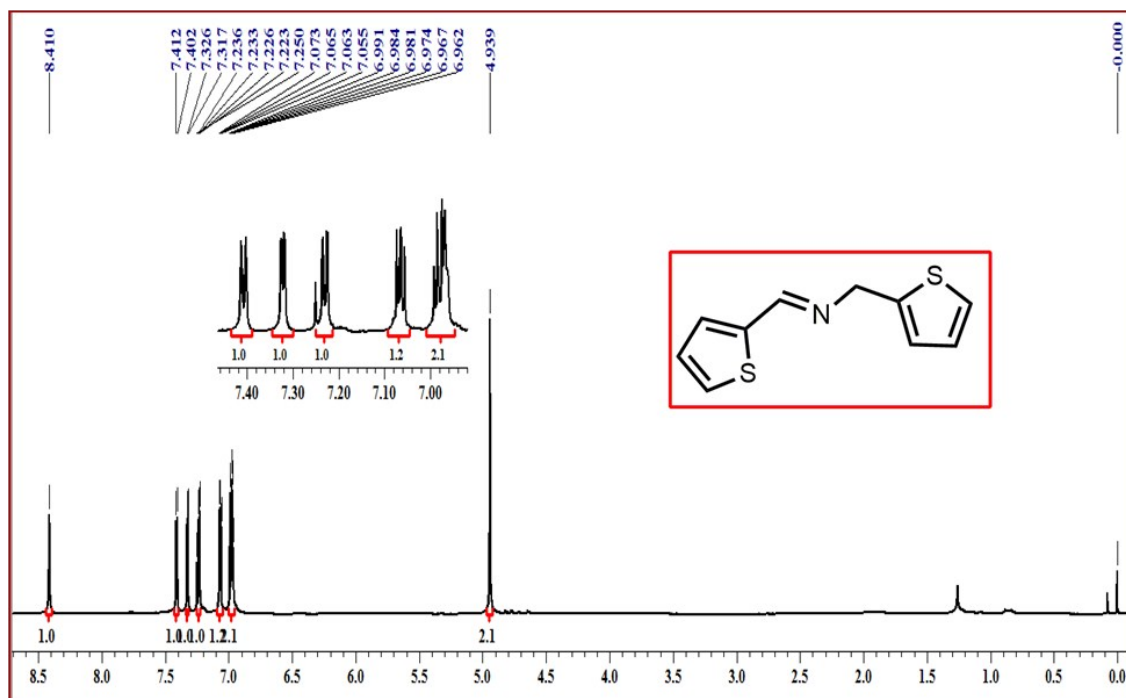
***N*-(3, 4-dichlorobenzylidene)-1-(3, 4-dichlorophenyl)methanamine (Fig. S11):**



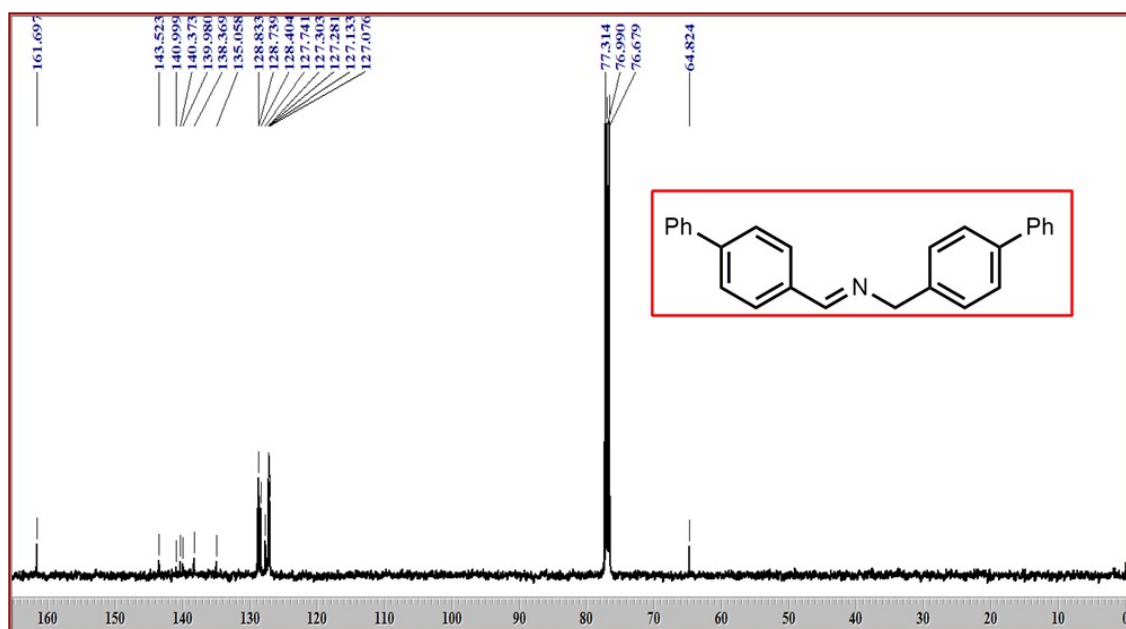
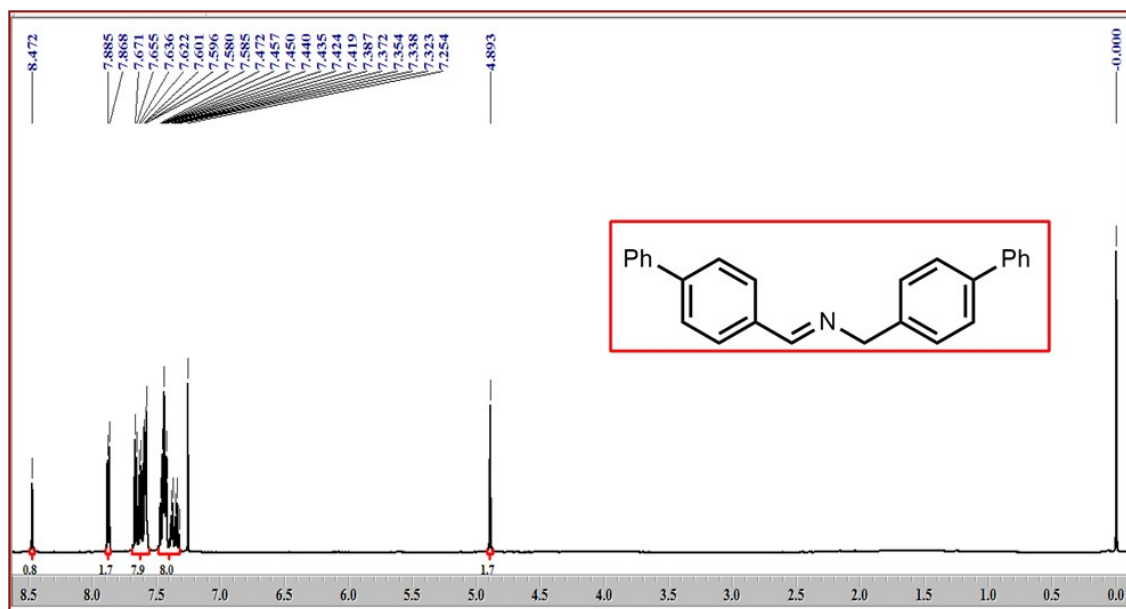
N-(1-naphthalenylmethylene)-1-naphthalenemethanamine (Fig. S11m):



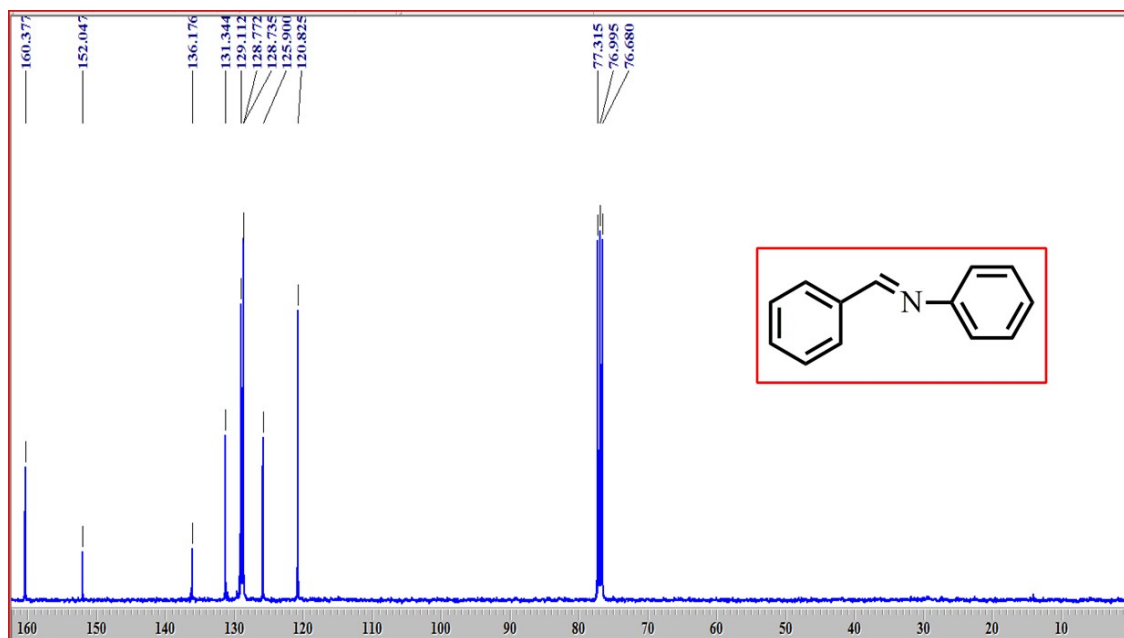
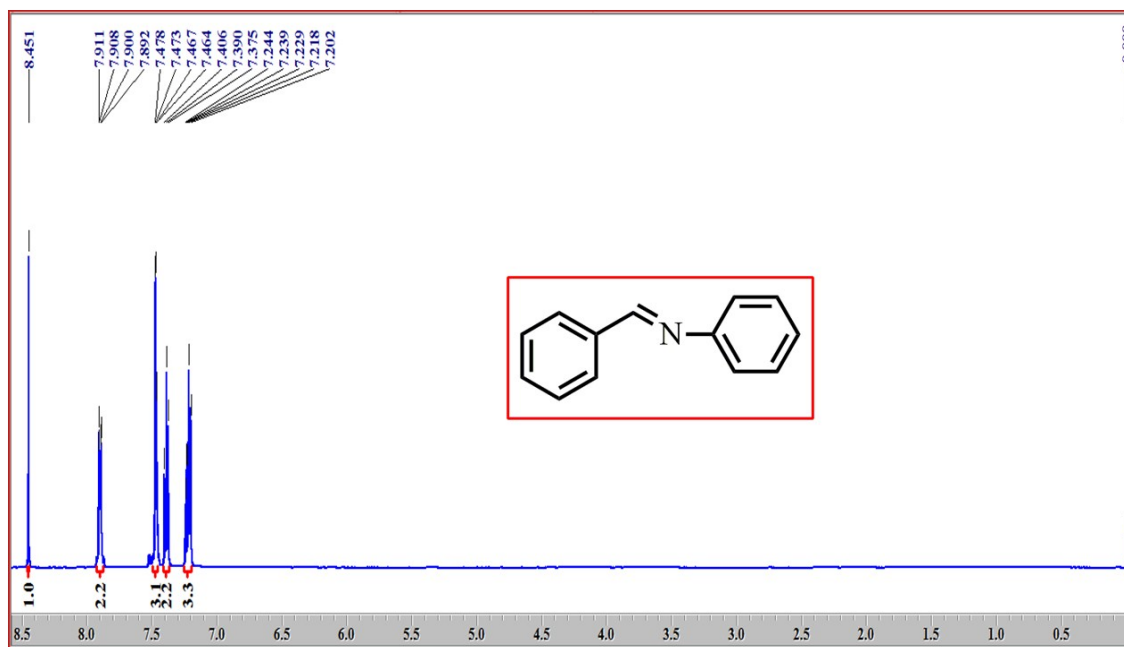
1-(thiophen-2-yl)-N-(thiophen-2-ylmethylene)methanamine (Fig. S11n):



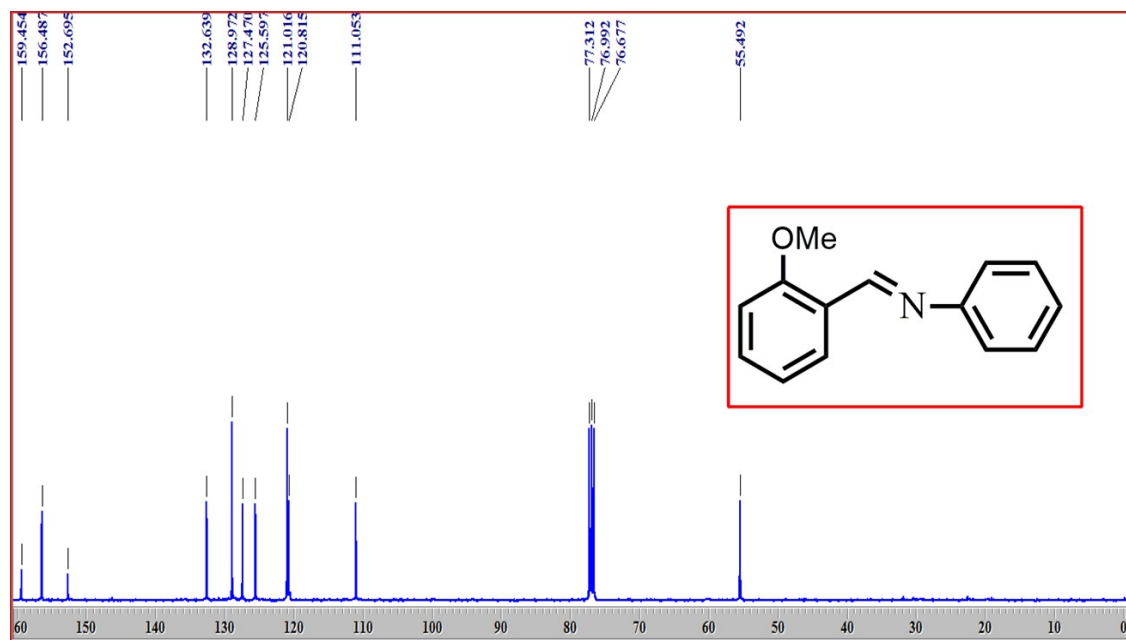
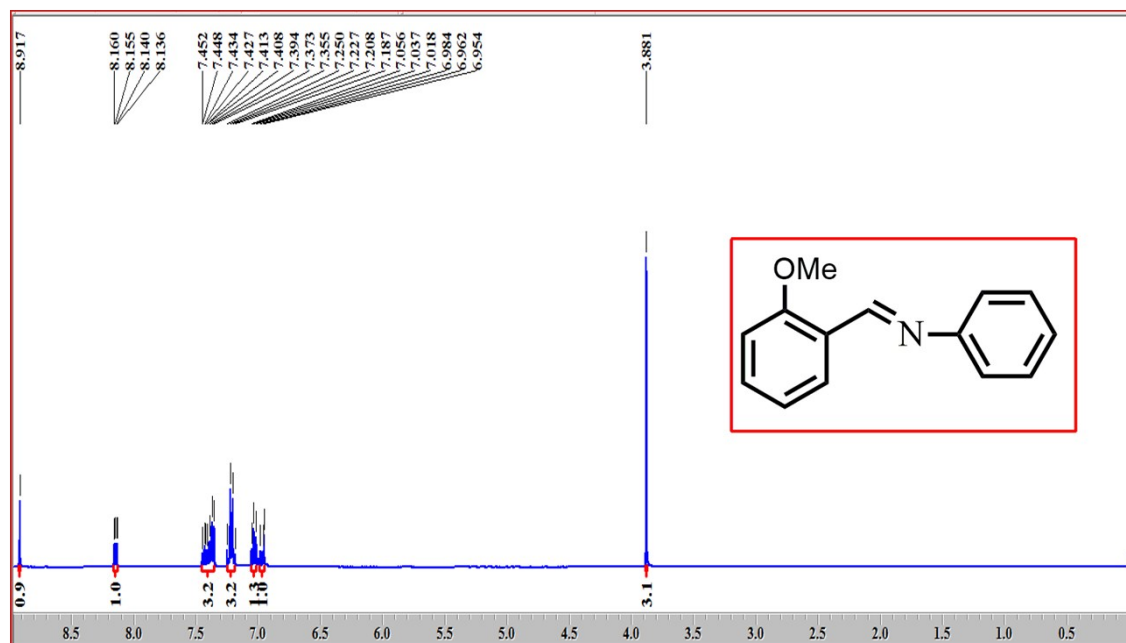
N-(1-biphenylmethylene)-1-biphenylmethanamine (Fig. S11o):



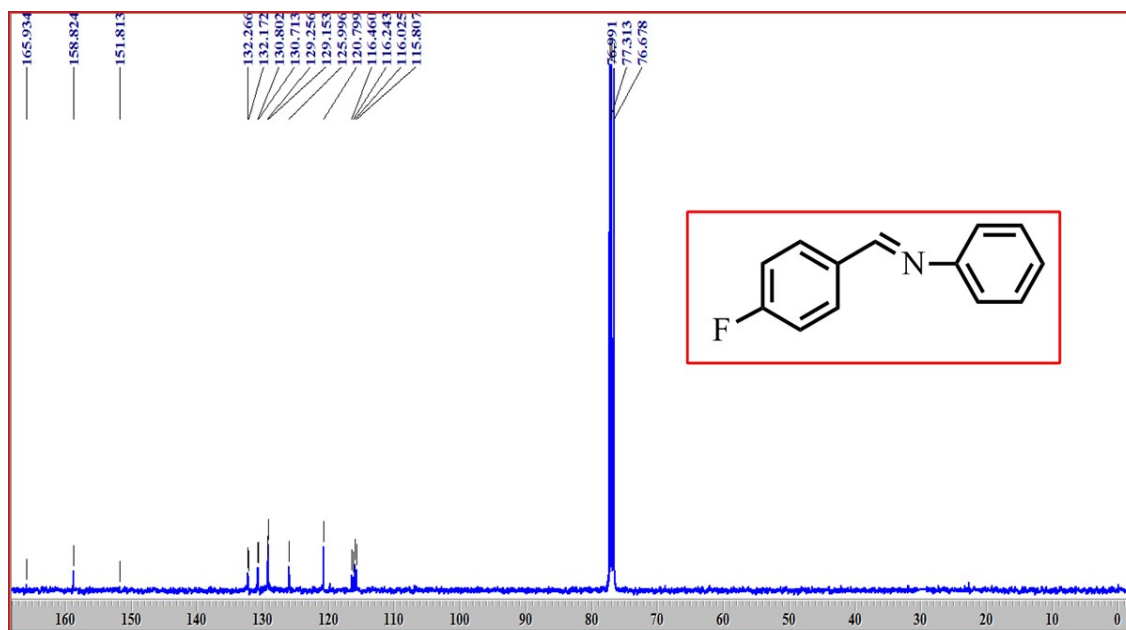
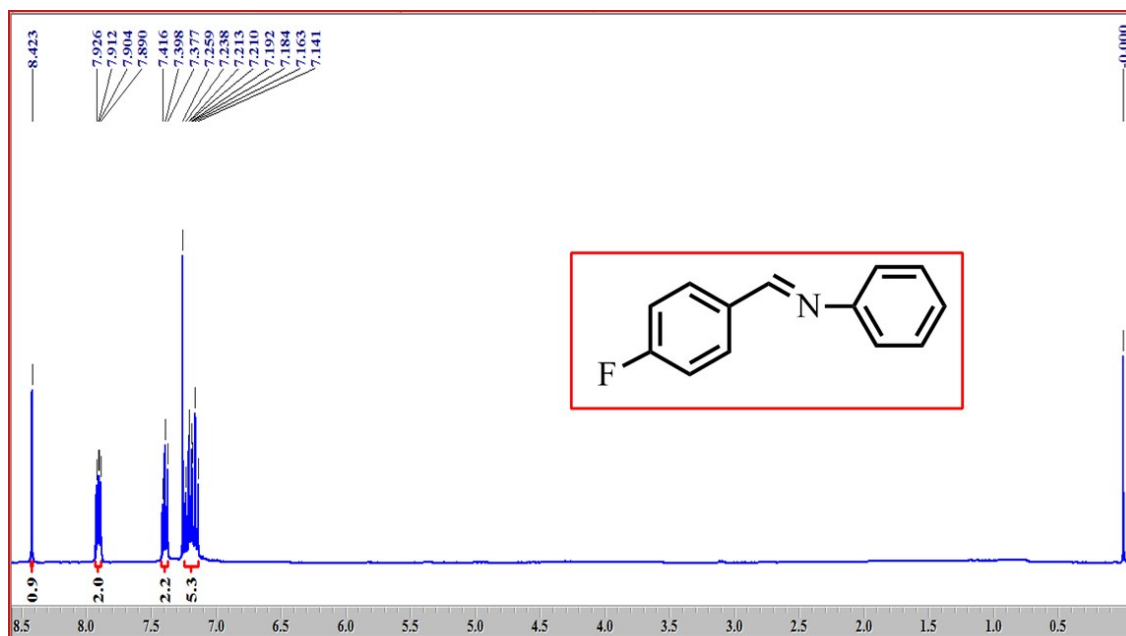
N-Benzylideneaniline (Fig. S11p):



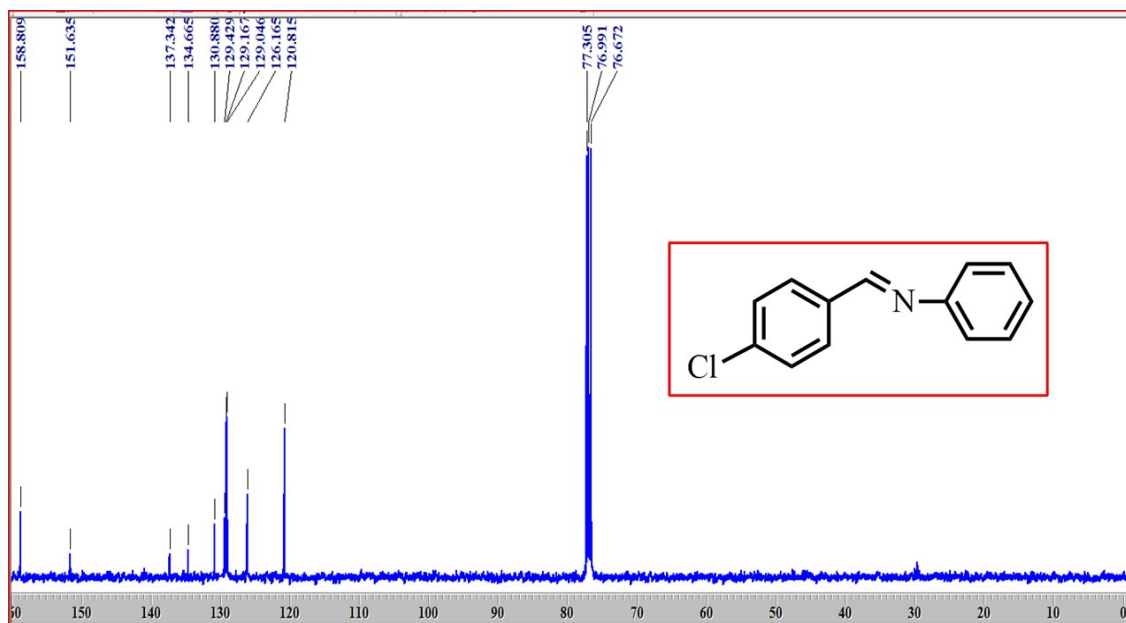
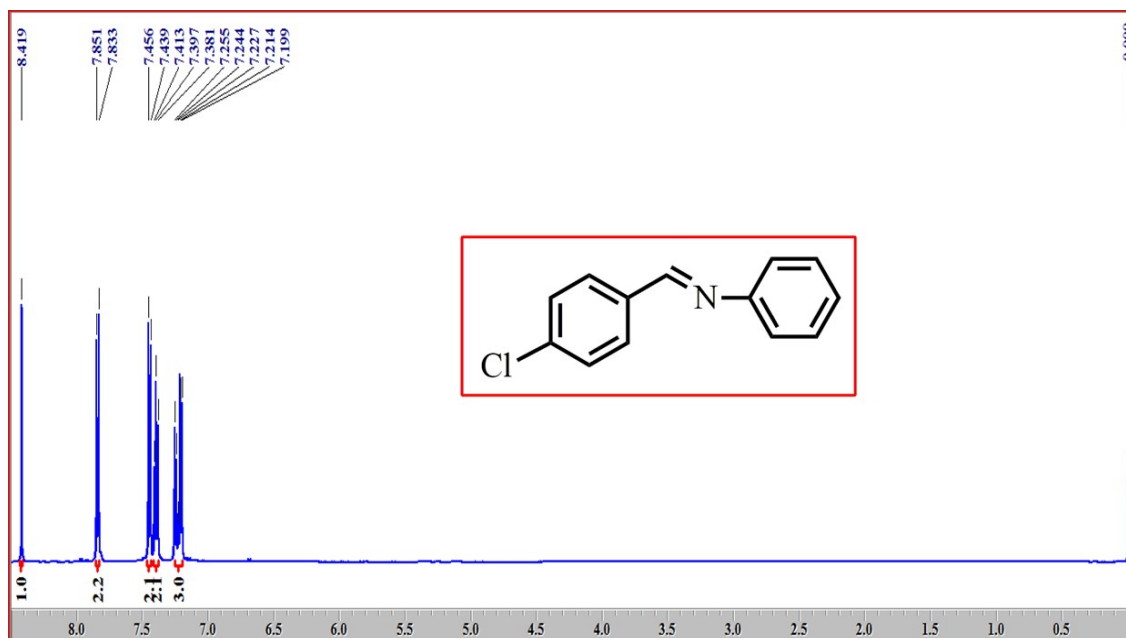
N-(2-methoxybenzylidene)aniline (Fig. S11q):



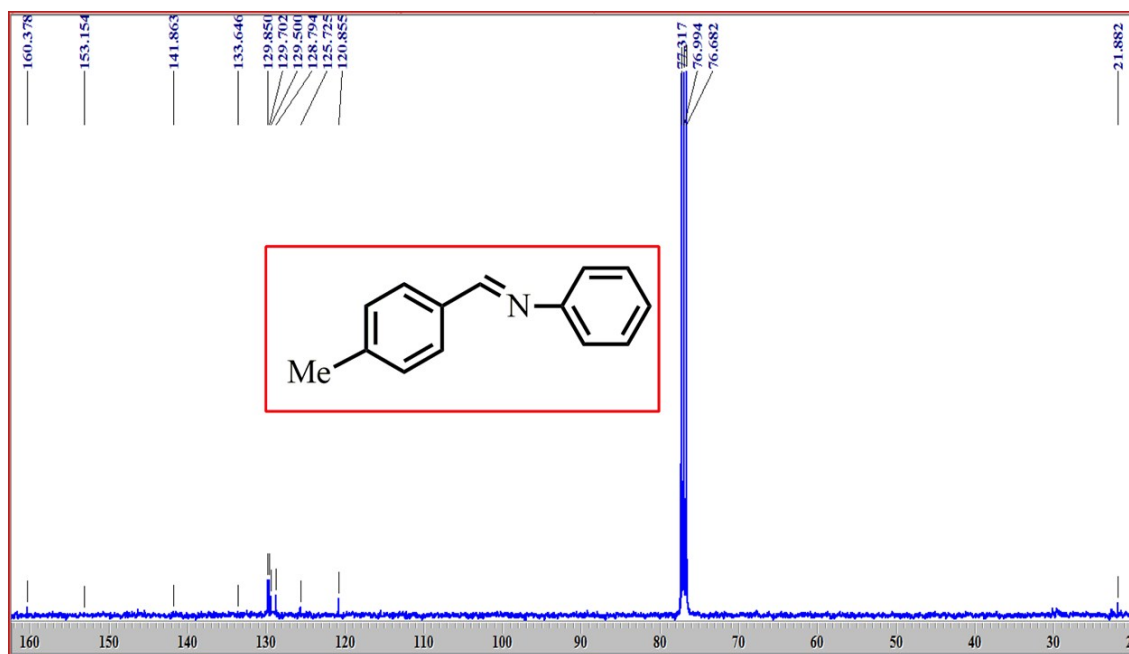
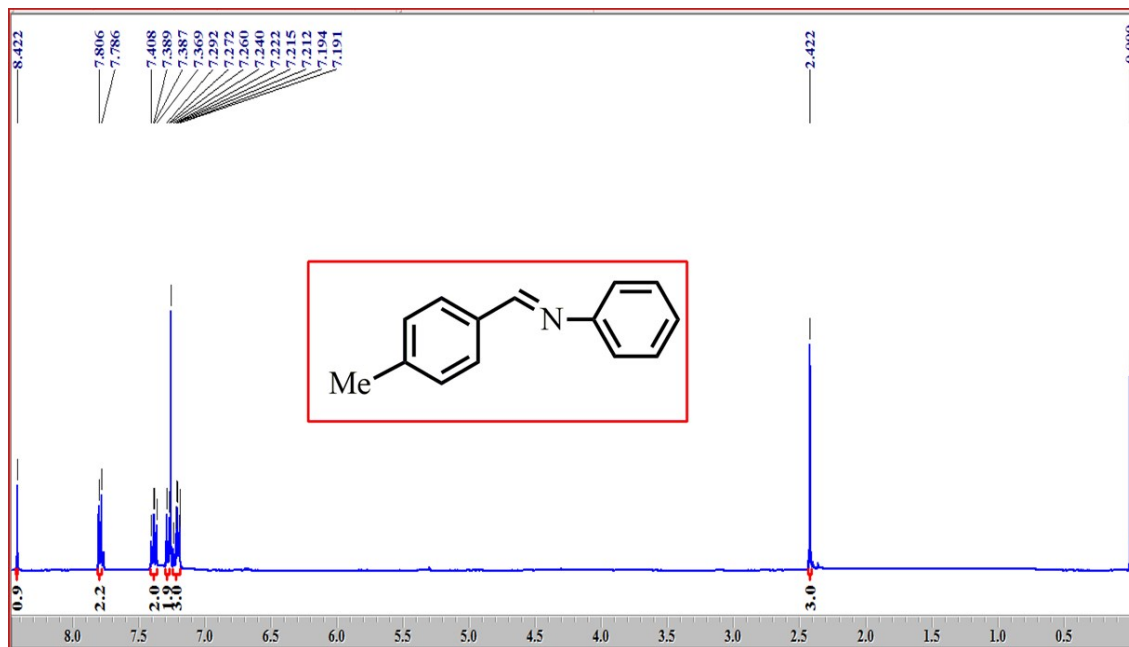
N-(4-Fluorobenzylidene)aniline (Fig. S11r):



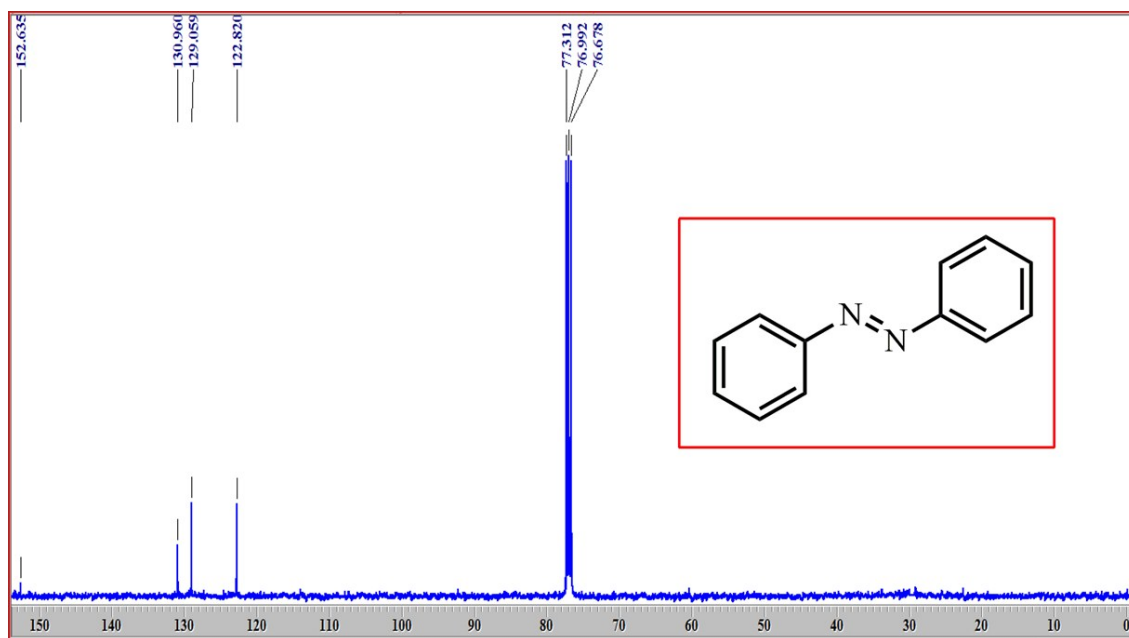
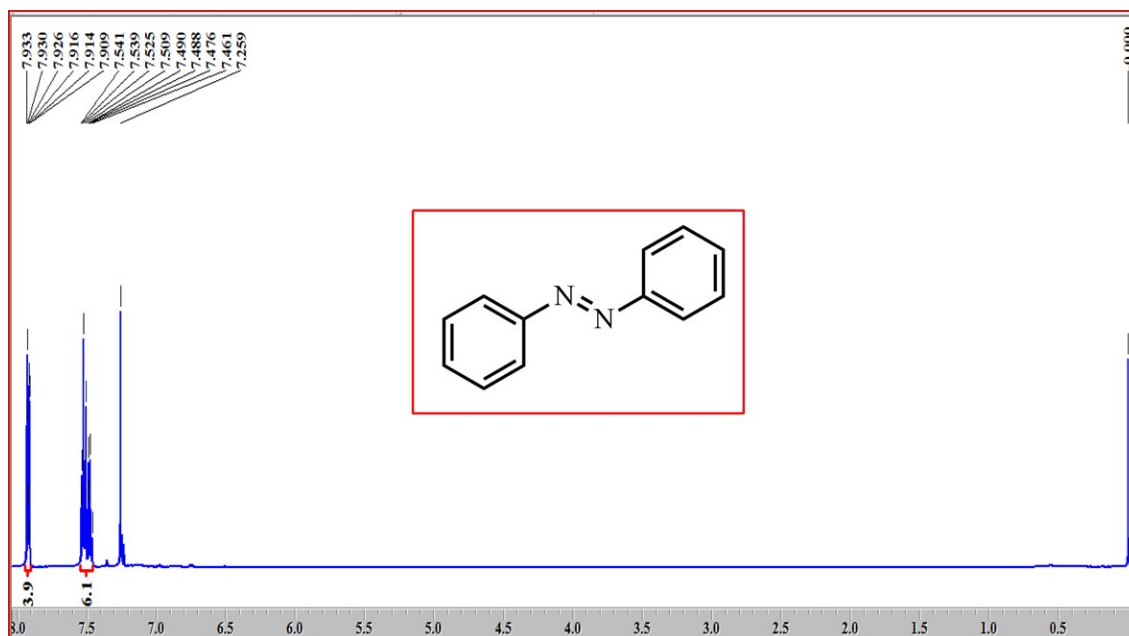
N-(4-Chlorobenzylidene)aniline (Fig. S11s):



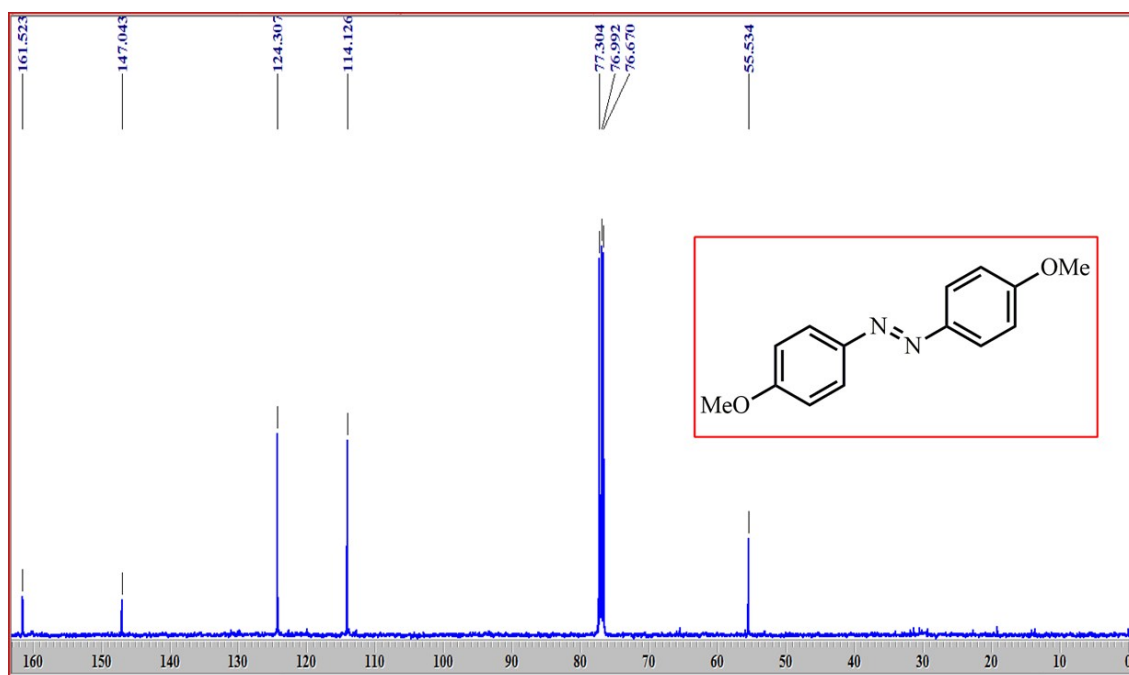
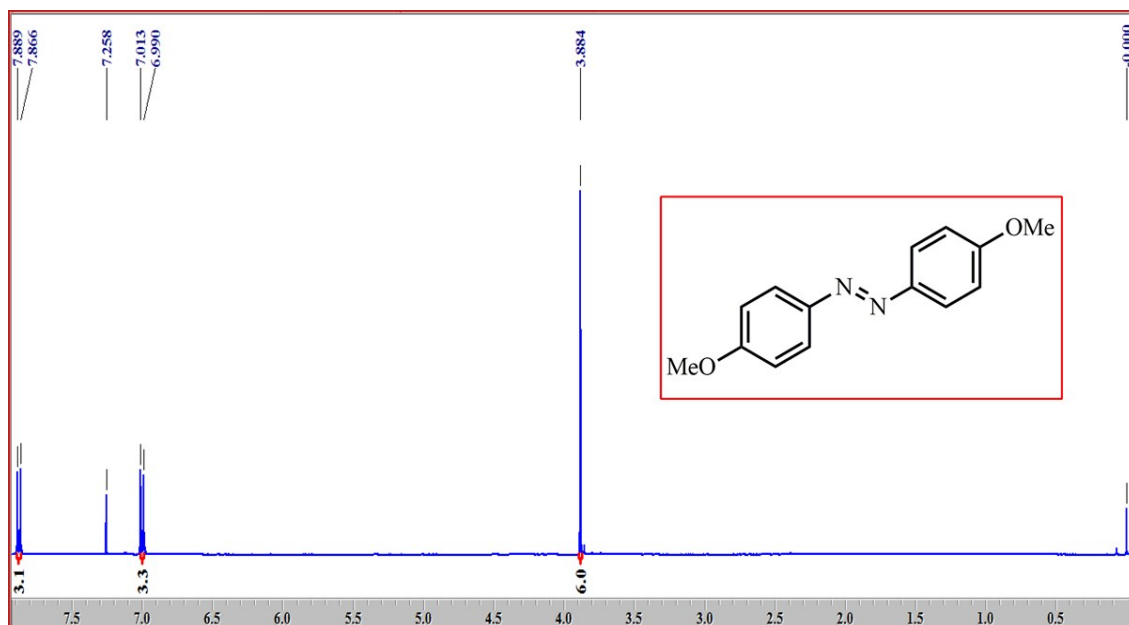
N-(4-Methylbenzylidene)aniline (Fig. S11t):



(E)-1,2-Diphenyldiazene (Fig. S11u):



(E)-1,2-Bis(4-methoxyphenyl)diazene (Fig. S11v):



(E)-1,2-Di-*o*-tolylidiazene (Fig. S11w):

